

AD-A108 601

PHYSICAL SCIENCES INC WOBURN MA
HIGH TEMPERATURE IN ABSORPTION MEASUREMENTS. (U)
SEP 81 R H KRECH, E R PUGH
PSI-TR-279 AFRPL-TR-81-79

F/G 20/5

F04611-80-C-0042

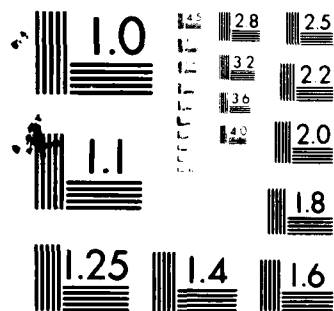
NL

UNCLASSIFIED

AFRPL-TR-81-79

$$\begin{array}{ccc} & | & \\ \mathbb{Z}_2 & \hookrightarrow & \mathbb{Z}_2 \end{array}$$

END
DATE
FILMED
1 82
DTIC



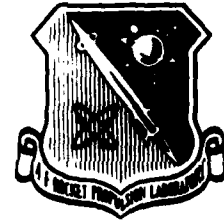
MICROCOPY RESOLUTION TEST CHART
NATIONAL BUREAU OF STANDARDS-1963-A

LEVEL II

12

AFRPL-TR-81-79

PSI TR-279



HIGH TEMPERATURE in ABSORPTION MEASUREMENTS

AD A108601

Authors: Robert H. Krech
Evan R. Pugh

Physical Sciences Inc.
30 Commerce Way
Woburn, MA 01801

September 1981

APPROVED FOR PUBLIC RELEASE; DISTRIBUTION UNLIMITED

The AFRPL Technical Services Office has reviewed this report, and it is releasable to the National Technical Information Service, where it will be available to the general public, including foreign nationals.

DTIC FILE COPY

Prepared for

AIR FORCE ROCKET PROPULSION LABORATORY
DIRECTOR OF SCIENCE AND TECHNOLOGY
AIR FORCE SYSTEMS COMMAND
EDWARDS AFB, CALIFORNIA 93523

DTIC
ELECTE
S DEC 16 1981 D
D

81 12 14 124

NOTICE

When Government drawings, specifications, or other data are used for any purpose other than in connection with a definitely related Government procurement operation, the United States Government thereby incurs no responsibility nor any obligation whatsoever; and the fact that the Government may have formulated, furnished, or in any way supplied the said drawings, specifications, or other data is not to be regarded by implication or otherwise as in any manner licensing the holder or any other person or corporation, or conveying any rights or permission to manufacture, use, or sell any patented invention that may in any way be related thereto.

FOREWORD

This report was prepared by Physical Sciences, Inc (PSI) for the Air Force Rocket Propulsion Laboratory, Edwards Air Force Base, California under Air Force Contract F04611-80-C-0042. The program was monitored by Curtis Selph of the Liquid Rocket Division.

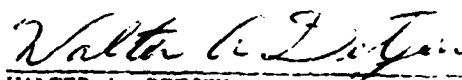
The work was performed by Robert Krech and Evan Pugh, with contributions by C. E. Caledonia, B. D. Green, P. Nebolsine, A. Pirri, D. Rosen, P. Lewis and N. Kemp of PSI.

This report has been reviewed by the Technical Information Office/TSPR and is releasable to the National Technical Information Service (NTIS). At NTIS it will be available to the general public, including foreign nations. This technical report has been reviewed and is approved for publication; it is unclassified and suitable for general public release.

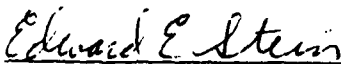
FOR THE DIRECTOR



CURTIS C. SELPH
Project Manager



WALTER A. DETJEN
Chief, Satellite Propulsion Branch



EDWARD E. STEIN
Deputy Chief, Liquid Rocket Division

UNCLASSIFIED

SECURITY CLASSIFICATION OF THIS PAGE (When Data Entered)

REPORT DOCUMENTATION PAGE		READ INSTRUCTIONS BEFORE COMPLETING FORM
1. REPORT NUMBER AFRPL-TR-81-79	2. GOVT ACCESSION NO. AD-9302402	3. RECIPIENT'S CATALOG NUMBER
4. TITLE (and Subtitle) HIGH TEMPERATURE IR ABSORPTION MEASUREMENTS		5. TYPE OF REPORT & PERIOD COVERED FINAL REPORT 15 AUG. 1980-30 JUNE 1981
7. AUTHOR(s) Robert H. Krech and Evan R. Pugh		6. PERFORMING ORG. REPORT NUMBER PSI TR-279
9. PERFORMING ORGANIZATION NAME AND ADDRESS PHYSICAL SCIENCES INC. 30 Commerce Way Woburn, MA 01801		8. CONTRACT OR GRANT NUMBER(s) F04611-80-C-0042
11. CONTROLLING OFFICE NAME AND ADDRESS Air Force Rocket Propulsion Laboratory Edwards AFB, CA 93523		10. PROGRAM ELEMENT, PROJECT, TASK AREA & WORK UNIT NUMBERS
14. MONITORING AGENCY NAME & ADDRESS (if different from Controlling Office)		12. REPORT DATE September 1981
		13. NUMBER OF PAGES 64
		15. SECURITY CLASS. (of this report) UNCLASSIFIED
		15a. DECLASSIFICATION/DOWNGRADING SCHEDULE
16. DISTRIBUTION STATEMENT (of this Report) PUBLIC RELEASE: DISTRIBUTION UNLIMITED		
17. DISTRIBUTION STATEMENT (of the abstract entered in Block 20, if different from Report)		
18. SUPPLEMENTARY NOTES		
19. KEY WORDS (Continue on reverse side if necessary and identify by block number) Laser propulsion, molecular coupling, CO ₂ lasers, absorption coefficient, H ₂ O		
20. ABSTRACT (Continue on reverse side if necessary and identify by block number) This is the final report on a research study entitled "High Temperature IR Absorption Measurements." The objective of this study was to measure the temperature dependence of the absorption coefficient of water vapor to determine the feasibility of using water vapor as a molecular seed to couple 10.6 μ CO ₂ laser radiation into a propellant for use in a high performance laser heated rocket thruster. A series of shock tube experiments were performed to determine the temperature dependence of the absorption coefficient of water vapor at high.		

DD FORM 1473 EDITION OF 1 NOV 65 IS OBSOLETE

UNCLASSIFIED

SECURITY CLASSIFICATION OF THIS PAGE (When Data Entered)

392405

xll

UNCLASSIFIED

SECURITY CLASSIFICATION OF THIS PAGE(When Data Entered)

temperatures on the P(16), P(18) and P(20) 10.6 μ CO₂ laser transitions. Measurements were made behind both incident and reflected shock waves encompassing a temperature range from 600 K to 3700 K at pressures from 1 to 40 atmospheres in 2, 5, and 10 mole percent water vapor in argon gas mixtures; a limited number of measurements were also made using 10 mole percent mixtures of water vapor in hydrogen or nitrogen. Conditions at several temperatures were sufficiently varied to investigate the effects of broadening on the absorption coefficient. Within the narrow spectral range from 944 to 948/cm covered in the measurements, no significant variation in the absorption coefficient was observed as a function of laser wavelength, water concentration, total pressure, or collision partner. These observations suggest that the water lines are sufficiently broadened to act as a continuum absorber under conditions to be found in a laser-heated rocket thruster. The measured laser high temperature absorption coefficients are 50 percent lower than the values obtained from the Ludwig empirical curve fit to low resolution data.

Accession For	
NTIS GRA&I	<input checked="checked" type="checkbox"/>
DTIC TAB	<input type="checkbox"/>
Unannounced	<input type="checkbox"/>
Justification	
By	
Distribution/	
Availability Codes	
Dist	Avail and/or Special
A	

UNCLASSIFIED

SECURITY CLASSIFICATION OF THIS PAGE(When Data Entered)

TABLE OF CONTENTS

<u>Section</u>	<u>Page</u>
1. Introduction	1
2. Previous Measurements	5
3. Experimental Technique	11
3.1 Advantages of Shock Tube Technique	11
3.2 Shock Tube Operating Principles	11
3.3 Operating Constraints	13
4. Experimental Apparatus and Procedures	16
5. Experimental Results	23
6. Discussion	36
7. Water as an Absorber in the CW Rocket	41
8. Ammonia as a Propellant and Absorber	44
9. Summary and Conclusions	54
References	55

LIST OF FIGURES

<u>Figure</u>		<u>Page</u>
1.	Possible configurations for laser heated thrusters.	2
2.	a. Spectral emissivities of the 6.3 μ fundamental and portions of the rotational band of H ₂ O at 540, 1040, 1640, and 2200 K.	6
	b. Spectral emissivities of H ₂ O at 2200 K, taken with a NaCl prism.	6
3.	Selected experimental H ₂ O absorption data.	7
4.	UTRC experimental and theoretical H ₂ O absorption data.	9
5.	PSI laser absorption data collected for NASA Marshall.	10
6.	Shock tube operation.	12
7.	Schematic of shock tube gas handling system.	17
8.	Schematic diagram of the IR absorption measurement system.	19
9.	Comparison of experimental and calculated incident shock pressure ratios.	21
10.	Comparison of experimental and calculated reflected shock pressure ratio.	22
11.	Typical low temperature pressure trace.	24
12.	Typical low temperature laser absorption trace.	25
13.	Typical high temperature pressure trace.	26
14.	Typical high temperature laser absorption trace.	27
15.	Absorption vs. total pressure on P(18) laser line.	28
16.	Absorption vs. pressure of water for P(16) laser line.	29
17.	Absorption vs. pressure of water for P(18) laser line.	30
18.	Absorption vs. pressure of water for P(20) laser line.	31

LIST OF FIGURES (CONT.)

<u>Figure</u>		<u>Page</u>
19.	Absorption coefficient vs. temperature for P(16) laser line.	32
20.	Absorption coefficient vs. temperature for P(18) laser line.	33
21.	Absorption coefficient vs. temperature for P(20) laser line.	34
22.	Water absorption coefficient vs. temperature.	35
23.	Band model average rotational line spacing vs. temperature.	37
24.	Calculated collision broadening boundaries for test gas mixtures vs. temperature.	39
25.	PSI recommended values for H ₂ O absorption coefficient.	40
26.	Absorption length (L_{abs}) and specific impulse (I_{sp}) for H ₂ /H ₂ O mixtures vs. total chamber pressure.	42
27.	Performance and heating map for small thruster, R = 0.02 m.	43
28.	Equilibrium concentration of NH ₃ .	45
29.	NH ₃ decomposition after sudden heating.	47
30.	UTRC ⁴ measured NH ₃ absorption.	49
31.	UTRC ⁴ calculated NH ₃ absorption coefficient.	51

1. INTRODUCTION

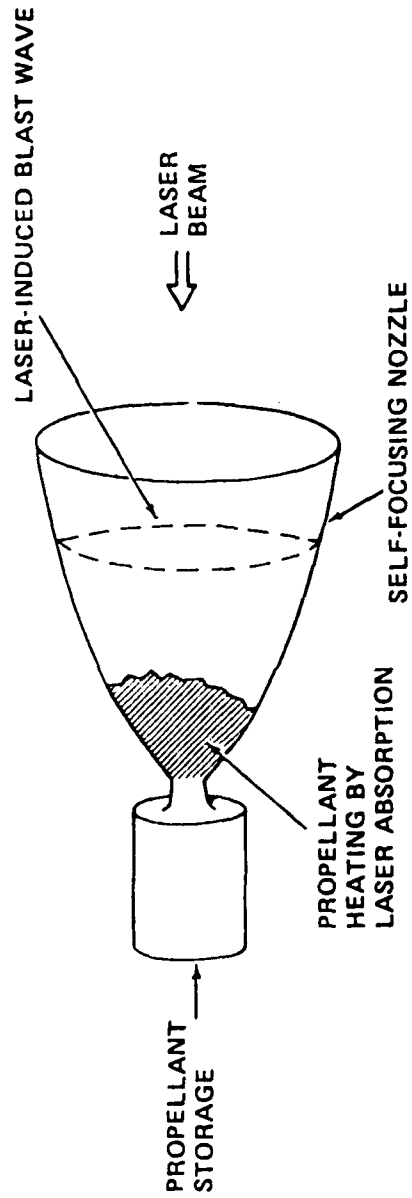
This report is the final report for a research study conducted at Physical Sciences Inc. for the Air Force Rocket Propulsion Laboratory at Edwards Air Force Base California under Contract F04611-80-C-0042 to determine the absorption coefficient of water vapor/propellant mixtures for laser propulsion and laser heated thrusters.

A laser-heated rocket-thruster converts laser energy, beamed from a remotely stationed laser, into thrust by using the laser radiation to heat the propellant. This technique provides a distinct advantage over conventional chemical rocketry by yielding a high specific impulse (greater than 1000 s vs. approximately 500 s for chemical rockets) at high thrust levels (potentially greater than 1000 lb); however, significant technological advances in the design and development of high power laser facilities, pointing and tracking systems, and collection optics will be required before laser-heated thrusters leave the laboratory. Either pulsed or continuous wave (CW) lasers can be used as the radiation source. Examples of each type of rocket are shown in Fig. 1. To obtain the highest specific impulse for a given temperature, hydrogen is the propellant of choice.¹⁻⁴ A 10.6 micron CO₂ laser is a potential candidate as the source of the laser radiation.

The only absorption mechanism for pure hydrogen at this wavelength is inverse bremsstrahlung, which requires the presence of electrons. Ionization of the hydrogen and the production of electrons is initiated only at temperatures between 7000 K and 11,000 K, depending on the pressure. Thus, pure hydrogen must be heated to absorb the laser energy.

In a pulsed laser propulsion system, this heating is accomplished by focusing the laser beam to create a laser-induced breakdown. The hot, rapidly expanding plasma drives a laser-supported detonation (LSD) wave into the

● REPETITIVELY PULSED LASER POWERED



● CONTINUOUS WAVE LASER POWERED

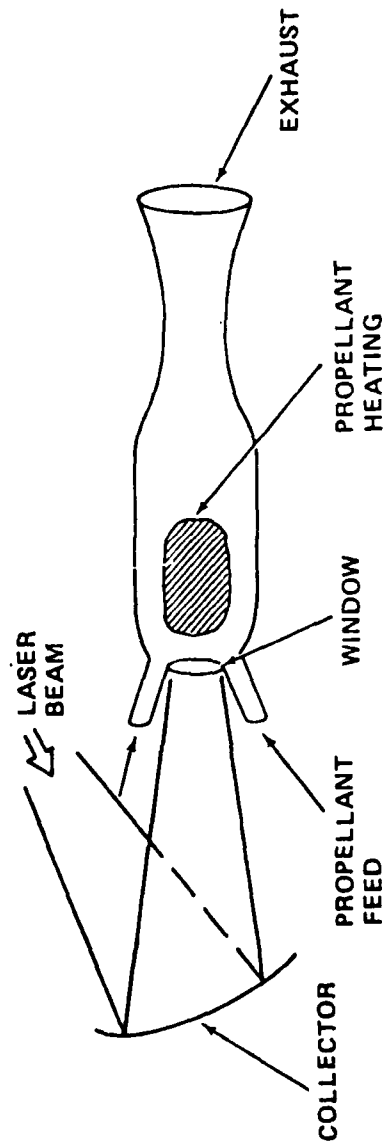


Fig. 1 Possible configurations for laser heated thrusters.

surrounding cool hydrogen.^{5,6} This gas is heated to extremely high temperatures around 20,000 K) and ionizes; and the electrons generated behind the LSD wave absorb the laser energy to sustain the propagation of the wave. The propagation of the wave continues until the intensity of the laser beam drops below the level required to sustain the wave or until the pulse ends. The heated gas then expands in the rocket nozzle creating thrust. Laboratory scale proof of concept experiments at 10.6 μ , yielding specific impulses over 1000 s, have been conducted at PSI and have demonstrated the feasibility of this system.^{5,6}

CW laser-heated thrusters with pure hydrogen propellant operate in a similar manner. In this thruster, when laser radiation is focused into a plasma, a laser-supported combustion (LSC) wave is created. If the gas flow velocity into the thrust chamber is matched to the wave velocity, then a stationary "flame" front is created. Hydrogen passing through the flame front is heated and ionized. The electrons generated by the ionization absorb by inverse Bremsstrahlung, and sustain the wave. One problem with this type of thruster is that there may be severe radiative heating of the chamber walls by the stationary 20,000 K plasma necessary to absorb the laser radiation. Seeding the hydrogen with an easily ionizable substance, such as cesium, has been proposed as one method to lower the operating temperature of the thruster and therefore reduce the heat load on the walls. If the hydrogen is seeded with a molecule that absorbs at low temperatures then the system is simplified. First, no LSC wave need be sustained to heat the hydrogen, allowing greater flexibility in the setting of gas flow rates. Second, and perhaps more important, the operating temperature is substantially lower and thus the heat load on the chamber walls is reduced. The problem is to find a low molecular weight, low temperature absorber that will not decompose to any significant degree below 3500 K to 4500 K the temperature range of a thruster operating with specific impulses between 1000 s and 2000 s.)

Water and/or ammonia have been proposed as possible candidates for absorbers at 10.6 μ . Water is particularly attractive since significant dissociation does not occur until the temperature exceeds 3500 K. In this program measurements were made on the 10.6 μ laser transitions P(16), P(18), P(20) found in high power CW CO₂ lasers to determine the absorption coefficient.

2. PREVIOUS MEASUREMENTS

A survey of the literature reveals a vast number of experimental measurements of the emission spectra of water. Until recently the primary interest in the spectra was the infrared signatures emanating from rocket exhaust plumes. In a number of papers on the subject, Ludwig and co-workers have compiled, reworked and theoretically analyzed the low resolution infrared spectra of hot water vapor.^{8,9,10} An example of their spectra is shown in Fig. 2.

The spectral region of interest in our study is narrow, 944 cm^{-1} to 948 cm^{-1} , encompassing the P(16), P(18) and P(20) $10.6\text{ }\mu\text{ CO}_2$ laser transition. Absorption in this region is due primarily to rotational transitions in the water molecule. The spectra shown in Fig. 2 reveals some structure in this wavelength region of interest but the 25 cm^{-1} resolution is not sufficient to ascertain the absorption coefficient at a specific laser transition.

The temperature dependence of the absorption coefficient can be estimated from low resolution measurements as shown in Fig. 3. The higher temperature values ($T > 1000\text{ K}$) come from the Ludwig empirical correlation.⁸ The intermediate values come from Penner's measurements.^{12,13}

In the lower temperature domain, the absorption is a continuum. The absolute coefficient has a quadratic dependence on H_2O pressure. The absorption at the lower temperature has been attributed to water dimers,¹⁴ $(\text{H}_2\text{O})_2$. These molecules are weakly bound and dissociate at a relatively low temperature. At room temperature the absorption coefficients have been measured at the lower frequencies of interest by Peterson and co-workers¹⁶ and the absorption coefficients are found to be very low, requiring a kilometer of path length to obtain significant absorption. Since water vapor will condense into liquid droplets if the vapor is saturated, any measurement must address the absorption by liquid water. The absorption depth of liquid water at

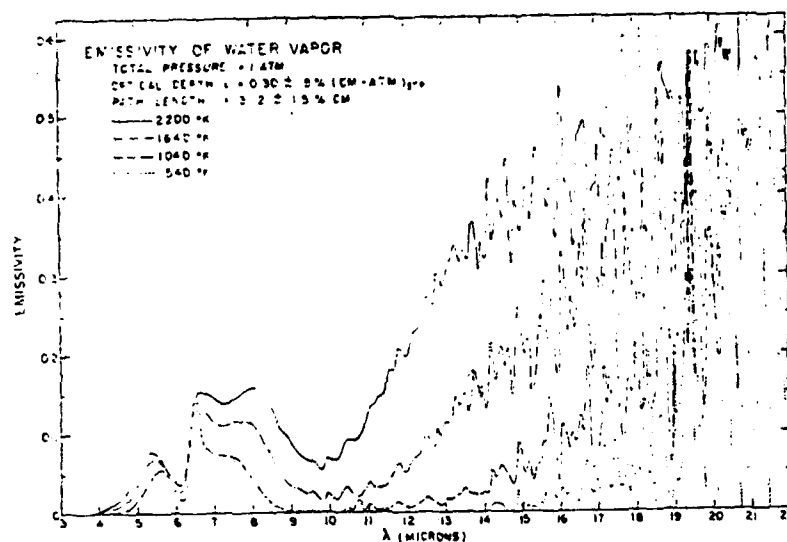


Fig. 2a) Spectral emissivities of the 6.3- μ fundamental and portions of the rotational band of H_2O at 540°, 1040°, 1640°, and 2200°K. (Ref. 10.)

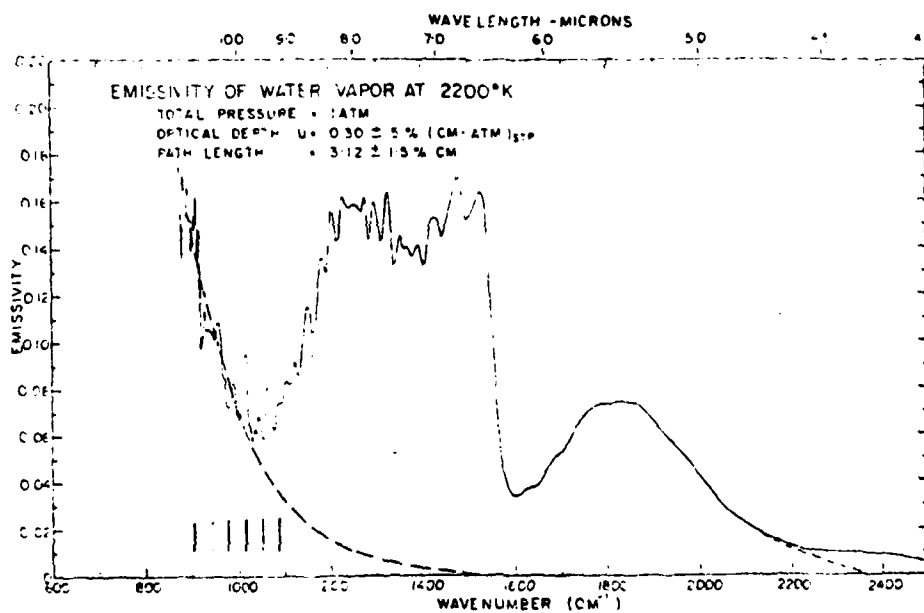


Fig. 2b) Spectral emissivities of H_2O at 2200°K, taken with a NaCl prism. Average spectral slit width = 25 cm^{-1} . The contour of the rotational band is indicated by a dotted line. (Ref. 10.)

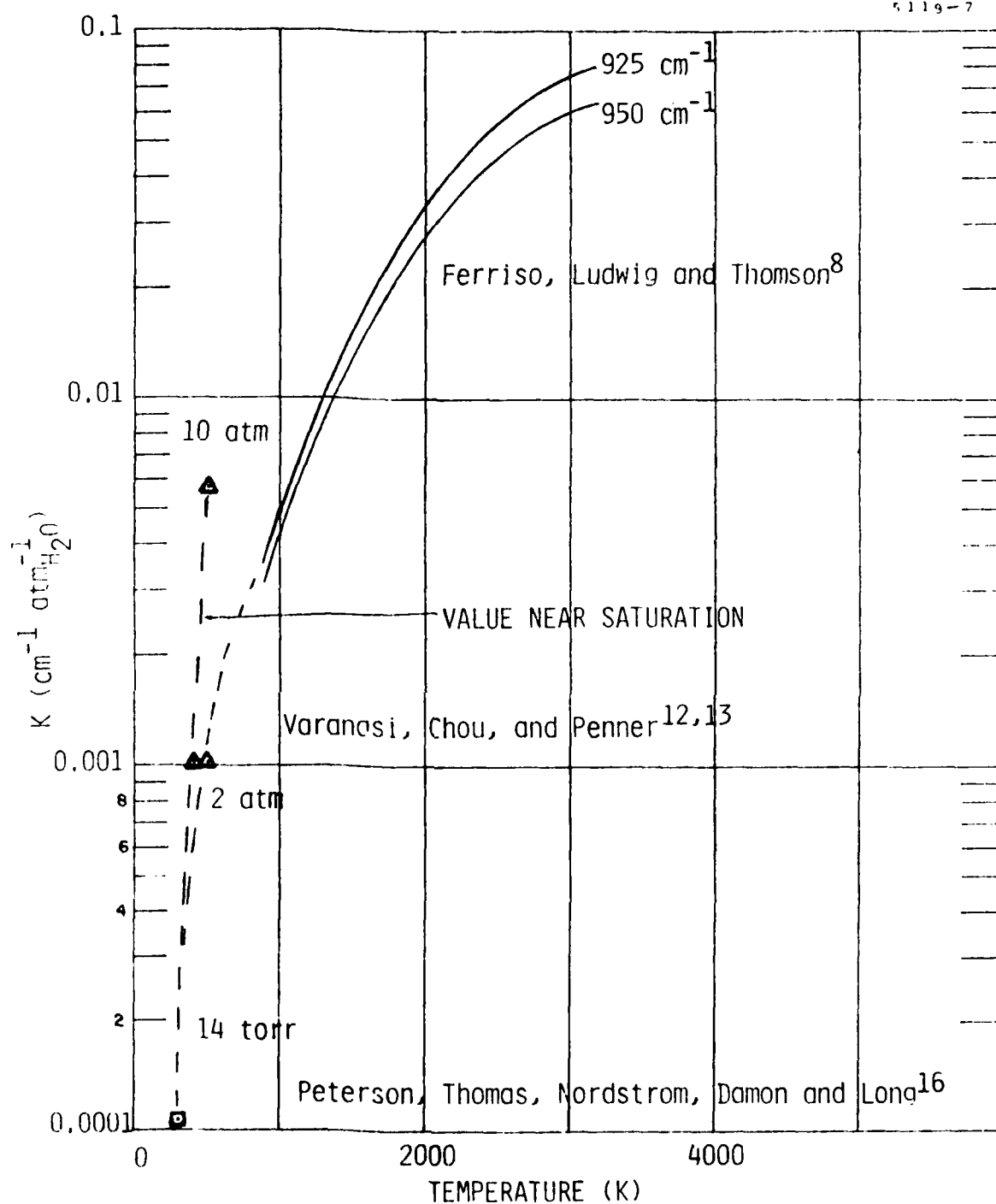


Fig. 3 Selected experimental H_2O absorption data.

10.6 μ is only several microns. If liquid water is present in the gas mixture then the measured absorption coefficient will be erroneously high; thus, the dotted line labeled "Value near saturation" in Fig. 3 represents the maximum absorption to be expected in pure water vapor.

Prior to this study there were two high temperature laser absorption coefficient measurements, one conducted by Fowler and co-workers at United Technologies Research Center⁴ and another at Physical Sciences sponsored by NASA Marshall Space Flight Center under Contract NAS8 33097.¹⁴

In the UTRC measurements a water vapor-hydrogen gas mixture was heated in a water cooled stainless steel flow reactor by a 7 kW CW CO₂ laser. Observations were made perpendicular to the heating laser by scanning through the hot plasma. The absorption coefficients obtained in these experiments are shown in Fig. 4, together with their predicted values. Their measurements yielded surprisingly large absorption coefficients, more than 10 times larger than those predicted by a rigid rotation model of the water molecule. If accurate, the higher value of the absorption coefficient would make water vapor the prime candidate as a seed absorber in a CW laser heated thruster propulsion system.

Physical Sciences conducted limited shock tube experiments to check the validity of using the Ludwig empirical absorption coefficients for water vapor in computer codes developed for NASA to predict the performance of laser heated thrusters.¹⁴ The results of the experiments, conducted in a shock tube using an untuned CW CO₂ laser, are shown in Fig. 5. The absorption coefficient obtained was 50% lower than the Ludwig empirical values. Thus, there existed an order of magnitude difference in the measured values of the absorption coefficient of water vapor at 10.6 microns. The present study seeks to reconcile these differences.

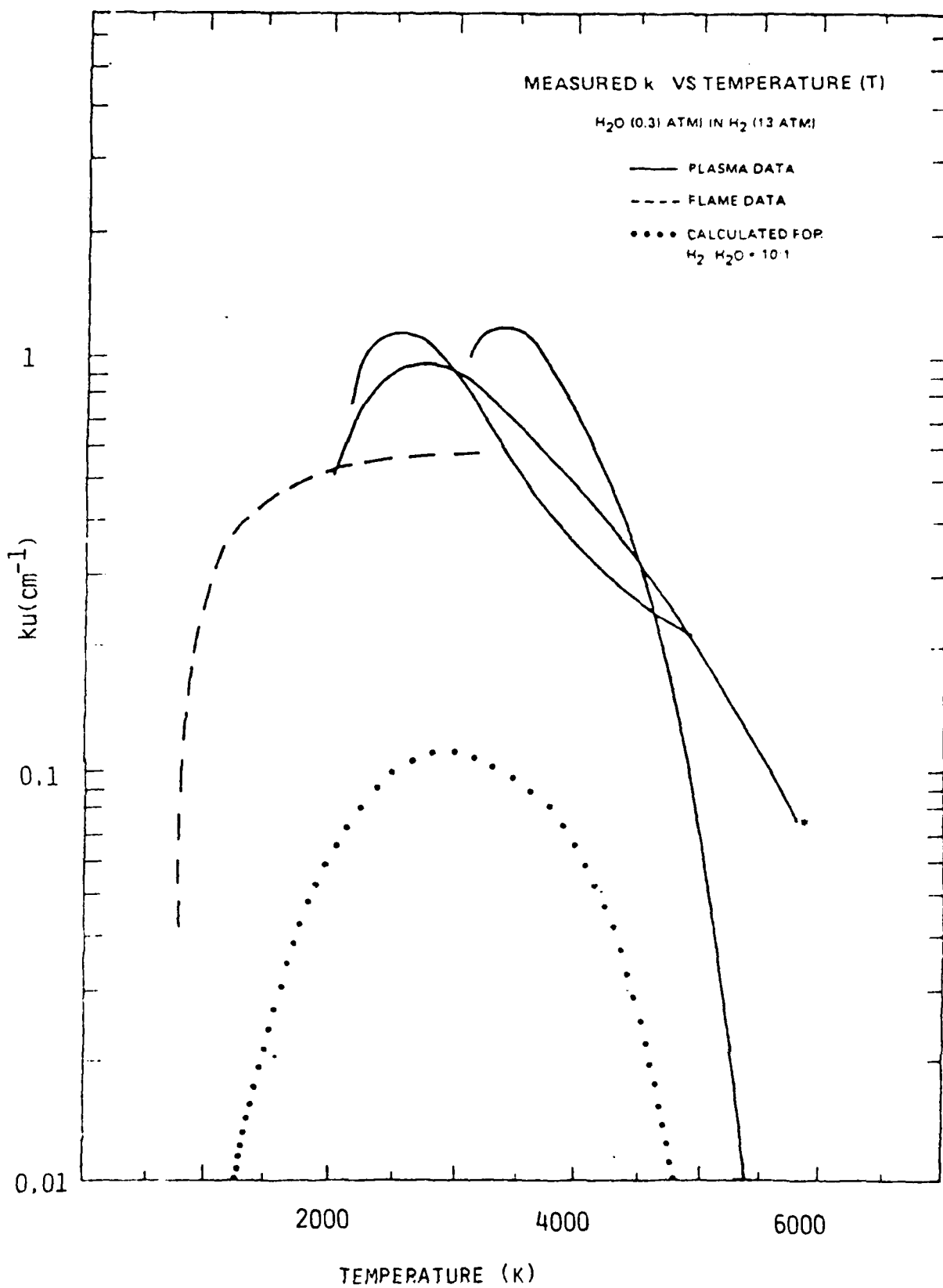


Fig. 4 UTRC experimental and theoretical H_2O absorption data.⁴

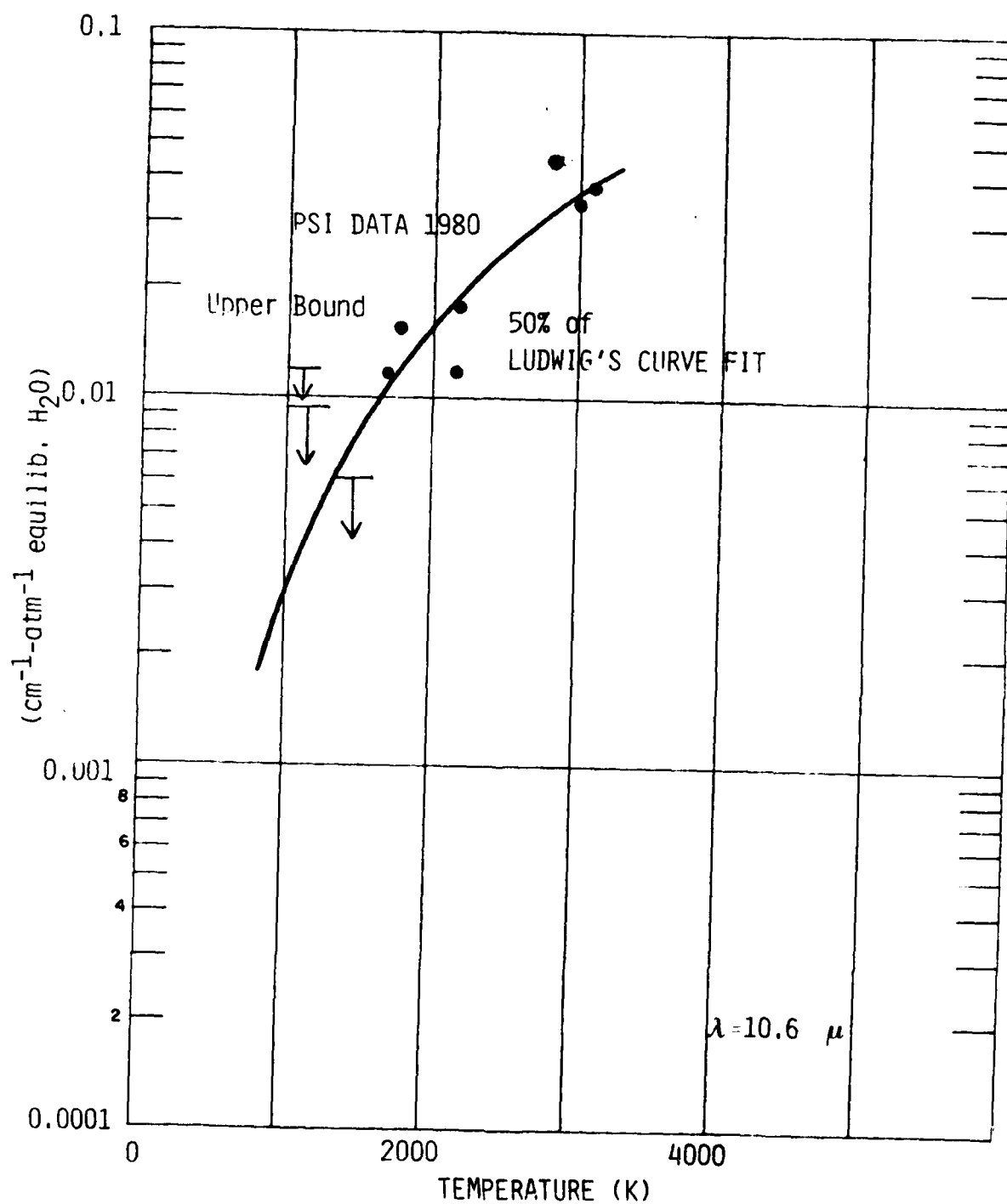


Fig. 5 PSI laser absorption data collected for NASA Marshall.¹⁴

3. EXPERIMENTAL TECHNIQUE

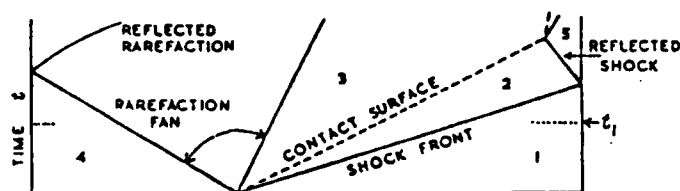
3.1 Advantages of Shock Tube Technique

The shock tube is a well understood experimental tool and is ideal for creating the pressures and temperatures required for the water vapor measurements. Using a furnace to produce the required temperatures becomes very difficult as the temperature is increased, and 3000 K is generally regarded as a practical upper limit. Electrical discharges can reach the required temperatures (up to 5000 K), but the resulting gas mixture is spatially nonuniform. In addition, the assumption of equilibrium chemistry in the resulting discharge is a poor assumption which complicates the data analysis. A flame can be used to create the required conditions, but it also exhibits nonuniform gas mixtures. In fact, flames usually contain large regions of cold gas which makes the interpretation of absorption data difficult. The shock tube takes the gas mixture almost instantly to a known high temperature and pressure. Test times up to a millisecond in duration can be attained, this is more than that required to simulate the heating process in a laser-heated thruster.

3.2 Shock Tube Operating Principles

As shown in Fig. 6, a shock tube consists of high pressure section and low pressure sections separated by a diaphragm. When the diaphragm bursts, the high pressure gas flowing into the low pressure section acts as a piston, compressing and accelerating the low pressure gas ahead of it. Compressing the low pressure gas is accomplished by a shock wave which travels ahead of the piston. When the shock wave reaches the end of the shock tube, where the test section is, it reflects off the end wall and reshocks the previously shocked gas, compressing more and stopping it. It is usual to specify the conditions in the high pressure region (the driver gas) by the subscript 4, conditions in the undisturbed low pressure section (the driven gas) by subscript 1, the gas conditions behind the incident shock wave by subscript 2

SHOCK TUBE OPERATION



Wave Diagram

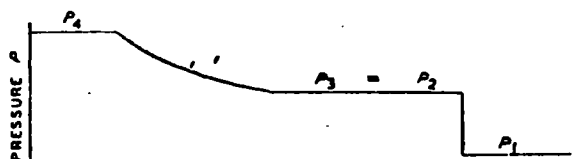
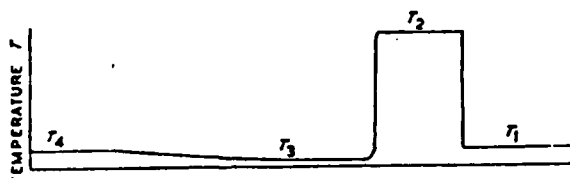
Pressure Distribution at time t_1 Temperature Profile at time t_1

Fig. 6 Shock tube operation.

and behind the reflected shockwave by subscript 5. This is shown in the position versus time plot (Fig. 6). Measurements are made in the test section in regions labeled 2 and 5.

The shock wave heats the processed (or driven) gas, resulting in an enthalpy per unit mass Δh , which is easily and accurately calculable when the shock velocity U_g is known. The approximation $\Delta h = U_g^2/2$ is accurate to within 10% for shock wave Mach numbers greater than four. The enthalpy of the processed gas is approximately doubled when the shock wave is reflected off the end wall. High temperatures require a high enthalpy/mass, thus implying high shock velocities. The velocity of the gas piston increases as the pressure ratio across the diaphragm increases but cannot exceed a value of a few times the initial sound speed in the driver gas ($U_{\text{piston}} < 2/(\gamma-1) a$, where γ is the specific heat ratio and a is the driver gas sound speed), even with an infinite pressure ratio. Therefore, driver gases with high sound speeds are desired. Most shock tube driver gases are, therefore, hydrogen or helium and in the PSI shock tube, room temperature hydrogen at up to 200 atmospheres pressure is used.

3.3 Operating Constraints

The initial pressure in the low pressure section is determined by the allowable range for the partial pressure of water vapor. The low pressure limit is determined from the requirements that any water vapor on the shock tube walls must not affect the measured water vapor mole percent of the gas in the tube. At low partial pressures of water vapor there may be a monolayer of H_2O vapor due to chemisorption, and we have estimated that van der Waals forces might also yield a monolayer of water vapor molecules on the shock tube walls. To eliminate any effect of this monolayer on the absorption measurement, we have calculated that the partial pressure of water vapor must be greater than 10^{-3} atm.

Similarly, if the pressure in the low pressure section is raised to the point where the vapor pressure of water exceeds the saturation vapor pressure at the coldest point in the system, water will condense out at that point, again making it difficult to control the amount of water in the tube.

Thus, absorption by water molecules condensed on the window, through which the absorption measurement will be made, places a limit on the permissible operating partial pressures of water. Liquid water has a large absorption coefficient for CO_2 radiation with a value of k_v greater than 10^3 cm^{-1} ; therefore, water must not be allowed to condense onto the windows. Although the initial gas sample will have a sufficiently low partial pressure of water, the shock wave raises this pressure by large factors. This is, of course, no problem in the middle of the shock tube where the gas is hot; however, the gas near the wall, which is at this same high pressure, is at or near the temperature of the wall. It is important that the initial partial pressure of the water not be greater than the saturation vapor pressure (corresponding to the window temperature) at the wall window temperature. This limit could have put serious constraints on the operating region. However, since the saturation vapor pressure of water is a steep function of temperature, heating the shock tube can overcome it. The vapor pressure of H_2O vapor as a function of temperature is as follows:

Vapor pressure p_g =	.02 atm @ 293 K
	.12 atm @ 323 K
	1.0 atm @ 373 K
	2.5 atm @ 400 K
	4.7 atm @ 423 K

A cold boundary layer, if thick enough, will absorb laser radiation in a manner different from the uniform hot gas in the center of the tube. It was necessary to estimate the contribution of this boundary layer to the overall absorption measurement.

The worst case for boundary layer interference occurs when the free stream temperature is 600 K, where the absorption coefficient is a minimum. Calculations for 20% water in hydrogen at a pressure of 50 atms indicated a boundary layer contribution of 12 percent. This contribution gets smaller rapidly as the temperature is raised and is negligible for temperatures greater than 1000 K.

4. EXPERIMENTAL APPARATUS AND PROCEDURES

The experimental absorption coefficient measurements were performed behind both incident and reflected shocks. The shock tube has a five foot long by 1.5 inch i.d. driver and a 15 foot long by 1.5 inch i.d. driven section. A schematic diagram of the shock tube is shown in Fig. 7. The optical measurements are made through anti-reflection coated zinc sulfide windows mounted one inch from the end wall in a five foot long by 1.31 inch square test section coupled to the driven section with a three inch long constant area transition piece. Shock pressure is measured by four piezoelectric transducers located at one foot intervals along the test section. The shock velocity is determined by the time of arrival of the shock wave at successive stations. The last transducer is located at the optical port to allow for a direct correlation of the optical signal with total pressure.

The shock heated gas mixtures consisted of 2 to 10 mole percent H_2O in either Ar, H_2 or N_2 . Extreme care went into the preparation and loading of the water vapor/gas mixtures to insure that the H_2O would not condense out and change the gas composition. The tube and all associated hardware were maintained at 320 K to permit the loading of up to 0.1 atm of H_2O vapor without condensation. (In actual practice, no more than 0.05 atm of H_2O vapor was loaded into the system.) Fresh gas mixtures were made for each run. The system was evacuated only to a vacuum of 1-10 μ to avoid removing the monolayer of water on the walls. Typically, the system was exposed to water vapor by filling and evacuating the tube several times just prior to the final fill before the shock to further stabilize the walls. No changes in pressure with time were observed either after making a mix and storing it in the mixing tank or after loading the gas in the shock tube prior to a test. Degassed, de-ionized water was stored in a flask attached to an end of the mixing tank as the source of water vapor. Typical H_2O partial pressures ranged from 16 to 30 torr depending on the mixture desired. The fill pressure was monitored by

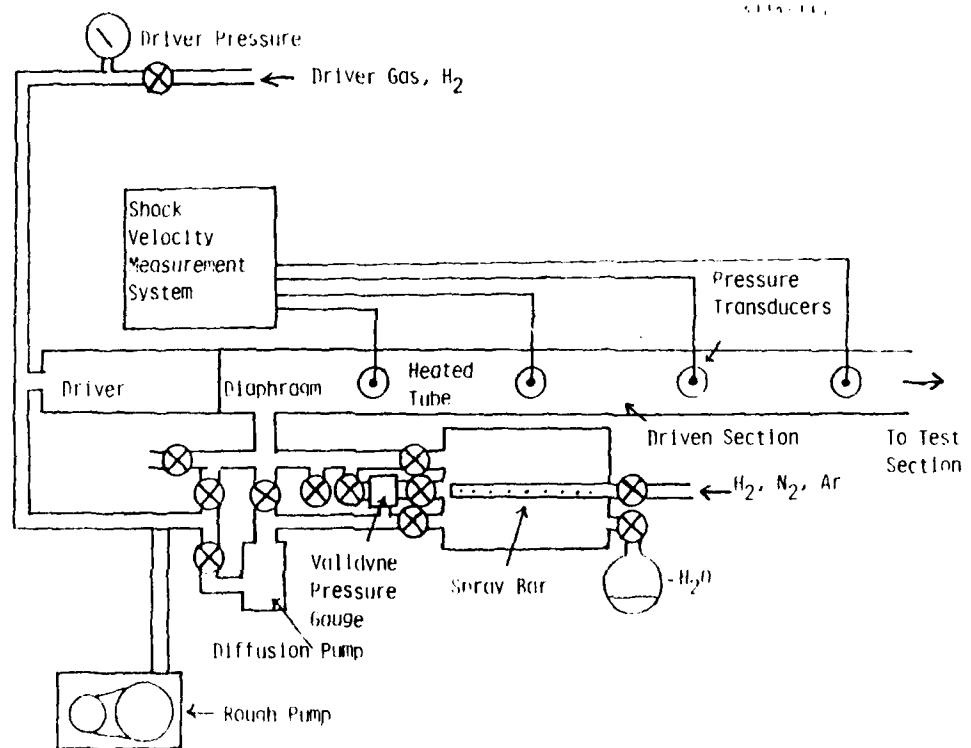


Fig. 7 Schematic of shock tube gas handling system.

a Validyne pressure transducer with a 0.2 torr sensitivity. Other gases were taken directly from the cylinder without further purification.

The stated minimum purities were: Ar, 99.996%, H₂, 99.995%, N₂, 99.99%. To insure good mixing in the mixing tank, the diluent gas was injected into the mixing tank through a spray bar running down the center of the tank. Twenty 0.040" holes on the bar at three inch intervals created swirling to promote rapid mixing.

A single-mode line-tuned CW CO₂ laser was used as the source of the laser radiation. A schematic diagram of the absorption system is shown in Fig. 8. The output beam was split into two components by a salt beam splitter. About 90% of the beam was directed to a salt diffuser located in front of the entrance window. This diffuser was employed to increase the sensitivity of the detection system by reducing refraction effects. Radiation from the exit window was collected by a germanium lens, and focused on an HgCdTe detector through a narrow band 10.6 μ interference filter (FWHM 0.15 μ). The filter was used to block out water emission at all but the laser wavelengths. No emission was observed within the laser bandpass when the laser was turned off as long as the filter was in front of the detector. The basic sensitivity of the absorption system is estimated to be around 0.2% for a 1:1 signal to noise level.

The remaining 10% of the laser radiation is sent through a 10 cm path-length absorption cell and into a Scientech laser power meter to determine the laser wavelength. The room temperature laser absorption coefficients of ethylene have been accurately measured,⁷ and by measuring the ethylene absorption coefficients it is possible to identify the laser transition without using a spectrometer.

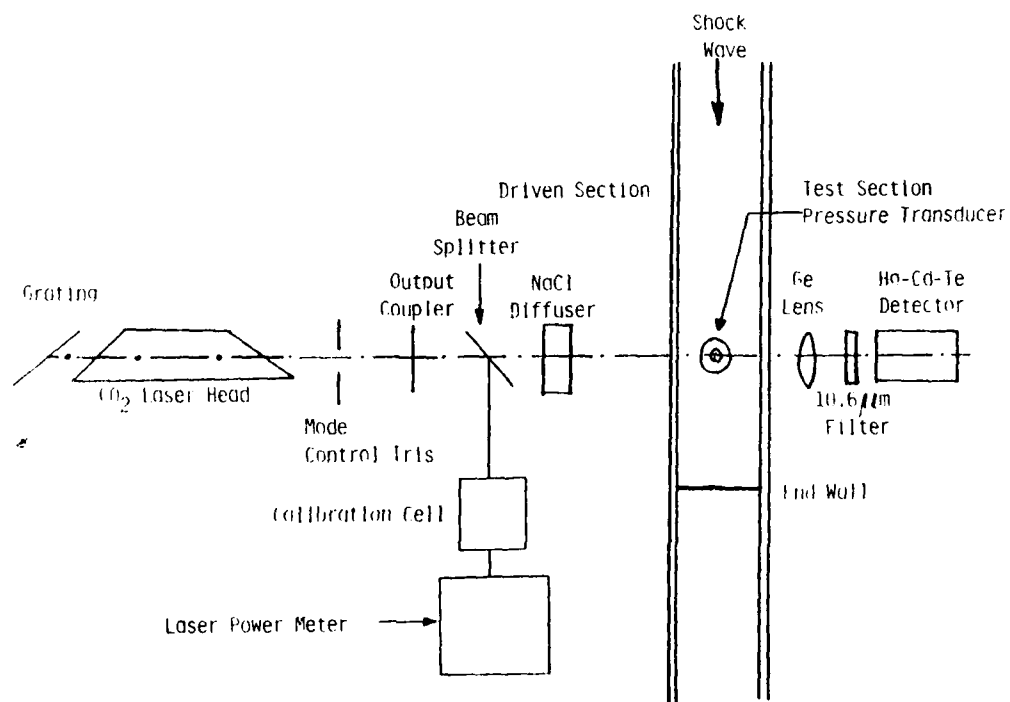


Fig. 8 Schematic diagram of the IR absorption measurement system.

The absorption coefficient α was determined using the measured optical transmission, I/I_0 , total pressure P , path length l , the initial mole fraction of H_2O , x_{H_2O} , and the calculated fractional dissociation at the equilibrium temperature, f_T by the following equation:

$$\alpha \frac{\text{cm}^{-1}}{\text{atm}} \frac{\text{atm}^{-1}}{x_{H_2O}} = \frac{\ln(I_0/I)}{f_T x_{H_2O} P \text{ atm } l \text{ cm}}$$

Temperatures behind the incident and reflected shocks were determined using the measured incident shock velocity, the initial pressure and gas compositions as input parameters to the PSI full equilibrium real gas shock program. Agreement between the calculated and measured shock pressure ratios was excellent, as is illustrated in Figs. 9 and 10.

Experimental data are collected and stored in a computer-controlled CAMAC based data acquisition system. The system is built around two LeCroy Waveform Digitizers. Each unit can simultaneously sample four analog signals at a 1 MHz rate, and has a 10-bit 32 K word memory that will store eight milliseconds of data. After a test, the data is transferred to a PRIME 400 computer for immediate preliminary analysis and storage.

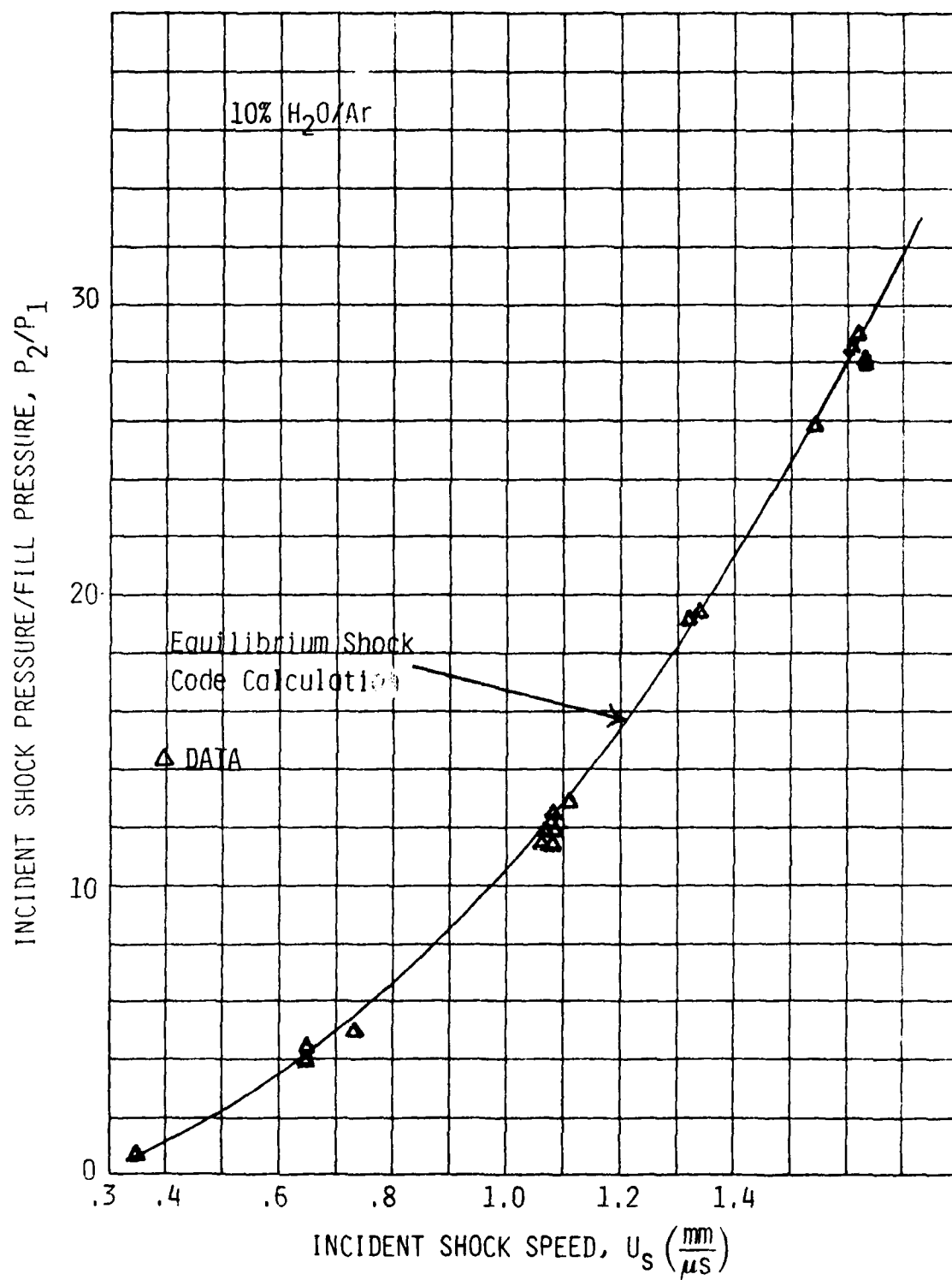


Fig. 9 Comparison of experimental and calculated incident shock pressure ratios.

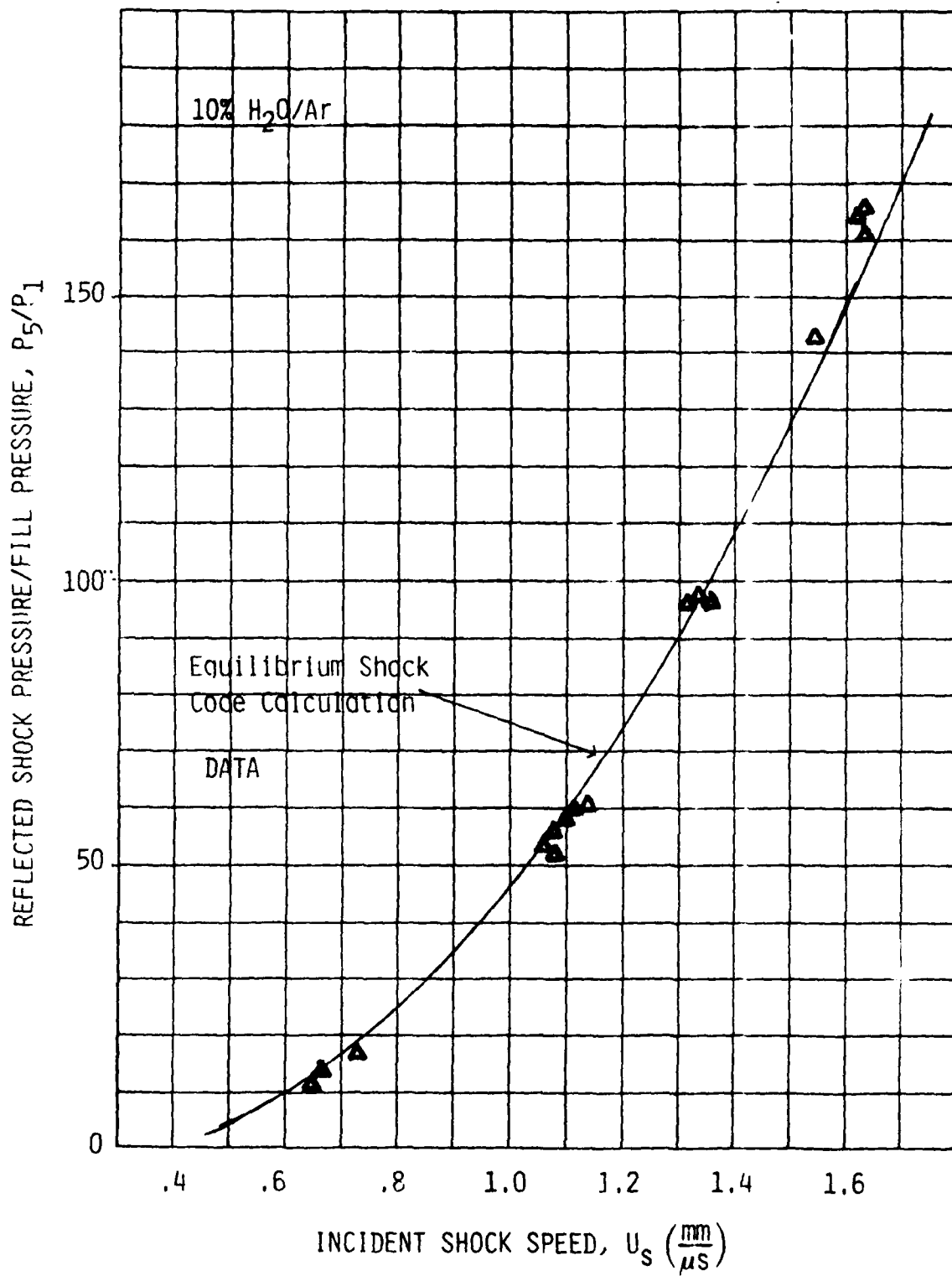


Fig. 10 Comparison of experimental and calculated reflected shock pressure ratio.

5. EXPERIMENTAL RESULTS

The majority of the tests were conducted using argon as the diluent gas instead of hydrogen, since it is much easier to drive a shock into a heavier gas. Measurements were made behind both incident and reflected shocks encompassing a temperature range from 600 K to 3700 K and at pressure from 1 to 40 atm in 2, 5, and 10 mole percent water vapor in argon gas mixtures. At the lower temperatures, little or no absorption was observed, particularly behind the incident shock where the pressures are low. Typical low temperature pressure and absorption data is shown in Figs. 11 and 12. At the highest temperatures, one third of the laser radiation was absorbed by the hot gas in the 3.31 cm pathlength. Typical high temperature pressure and absorption data are shown in Figs. 13 and 14.

At several temperatures the total pressure behind the shock, and the partial pressure of water in the gas was varied sufficiently to assess the effect of pressure and water vapor concentration on the absorption coefficient on each of the three laser transitions of interest. For example, there was no change in the value of the absorption coefficient for total pressures ranging from 5 to 40 atm at 2250 K on any of the laser transitions (see Fig. 15). At the same temperature, plots of $\ln I_0/I$ vs P_{H_2O} have a constant slope indicating that the absorption depends solely upon the line density of molecules in the laser path. No significant variations in the H_2O absorption coefficient were observed among the three laser transitions for a given temperature within experimental uncertainty. (See Figs 16, 17, 18.) Raw data collected on each of the laser transitions is shown in Figs. 19, 20 and 21.

Nine tests were conducted using 10% H_2O/H_2 gas mixtures between 600 K and 1400 K. These H_2O absorption coefficients fall within H_2O/Ar data collected in the same temperature range. Two tests with 10% H_2O/N_2 gas mixtures were also conducted on the P(18) CO_2 transitions and these also overlap the H_2O/Ar data. All the data collected along with the Ludwig empirical curve fit is plotted in Fig. 22.

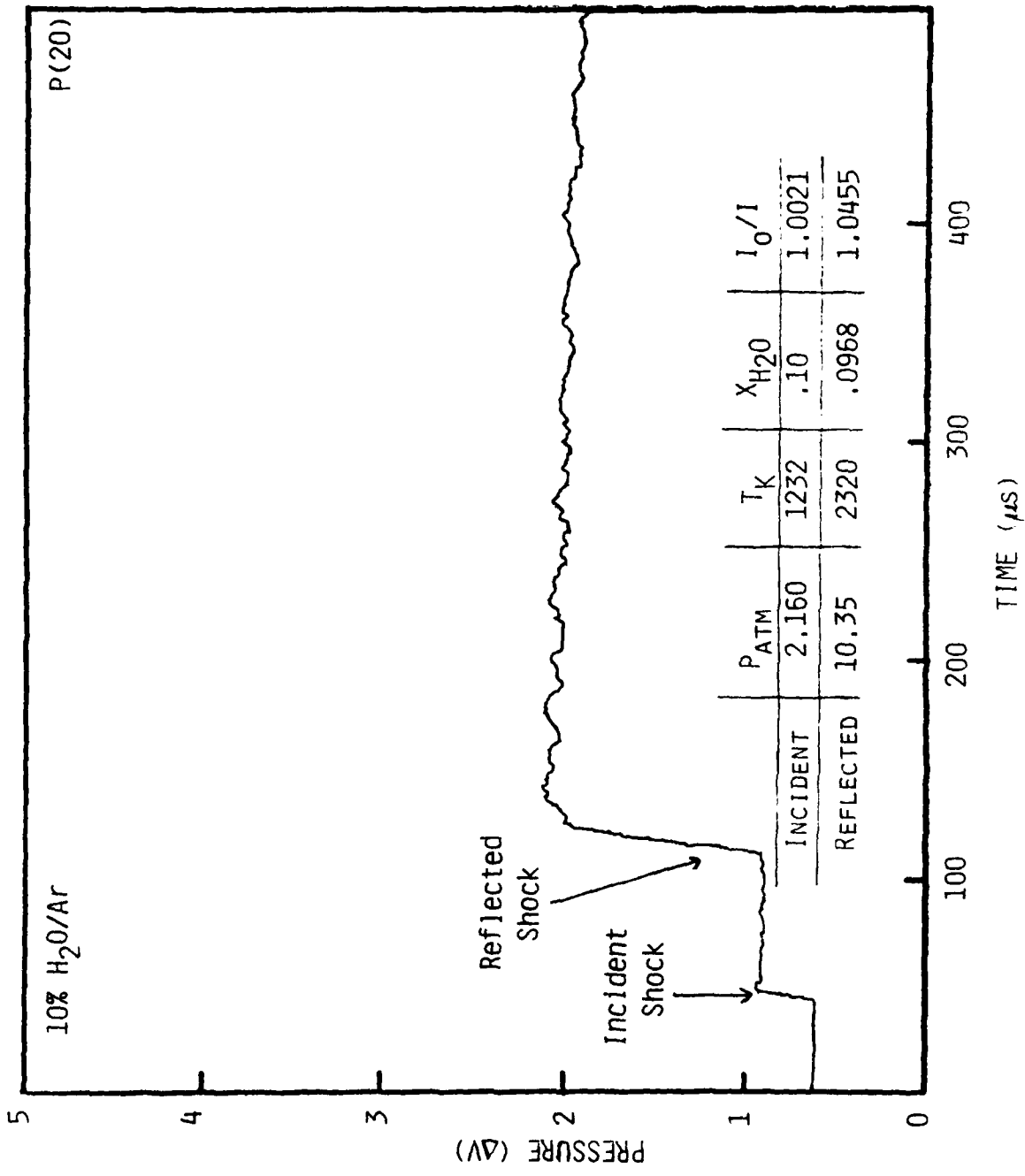


Fig. 11 Typical low temperature pressure trace.

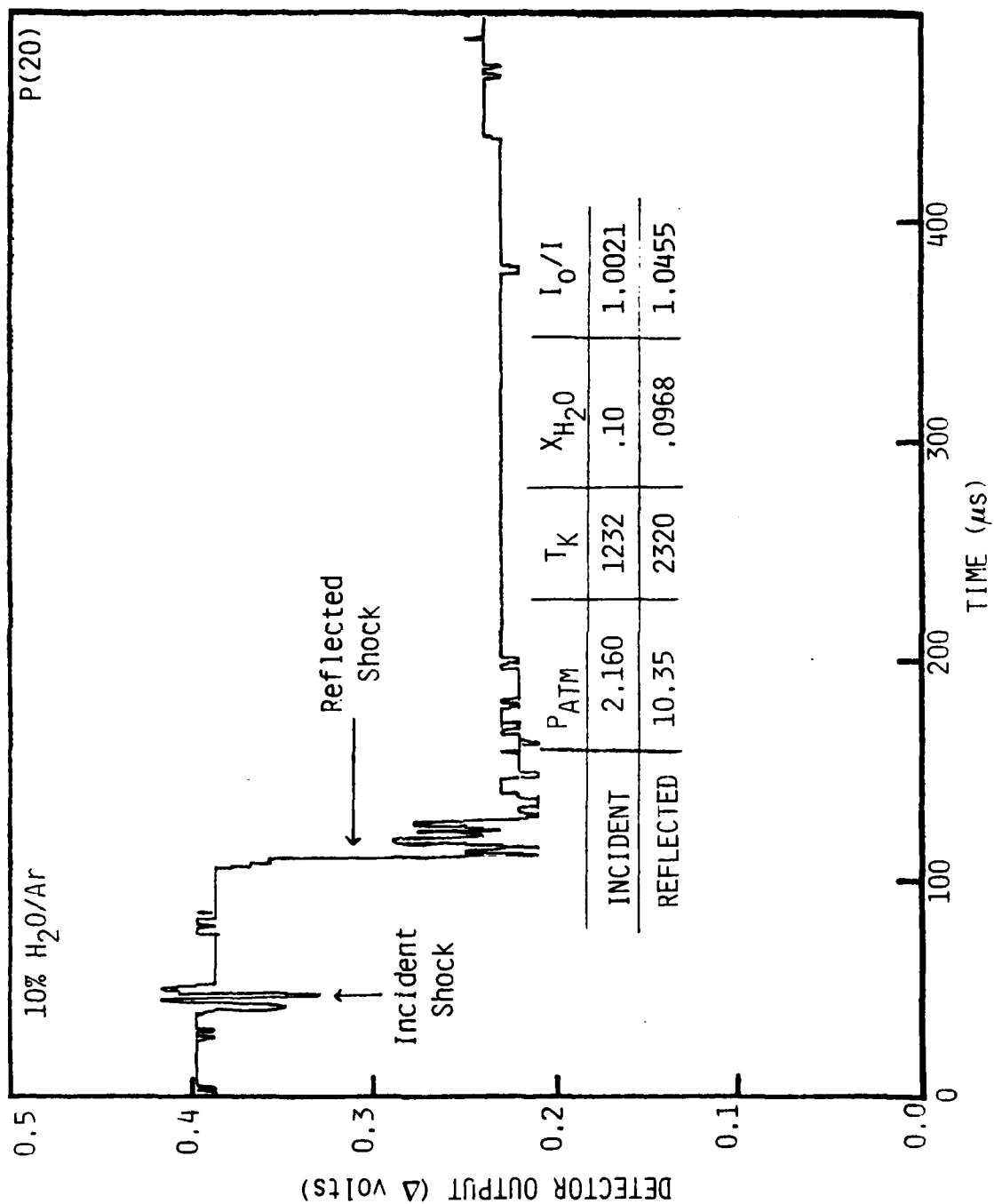


Fig. 12 Typical low temperature laser absorption trace.

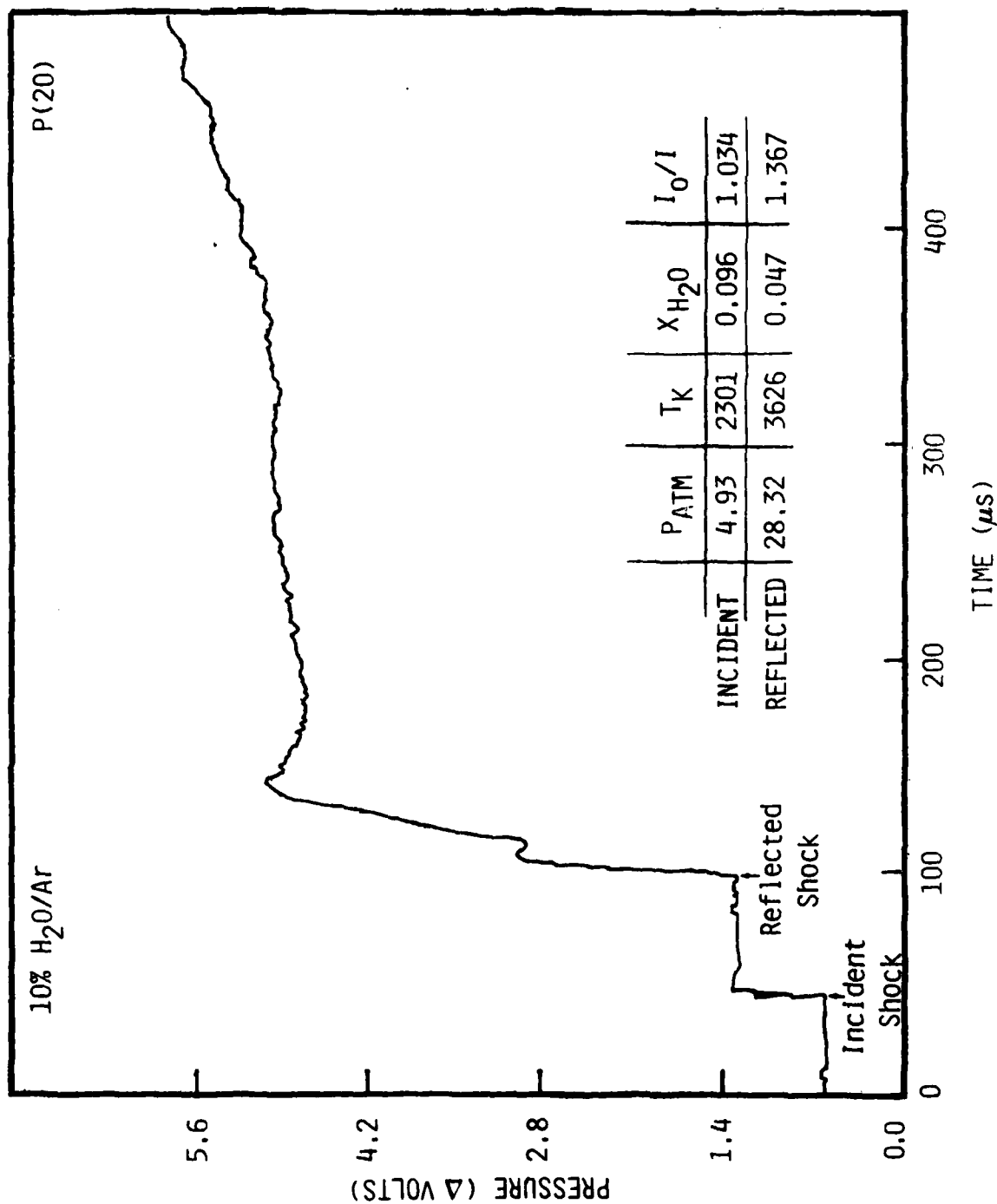


Fig. 13 Typical high temperature pressure trace.

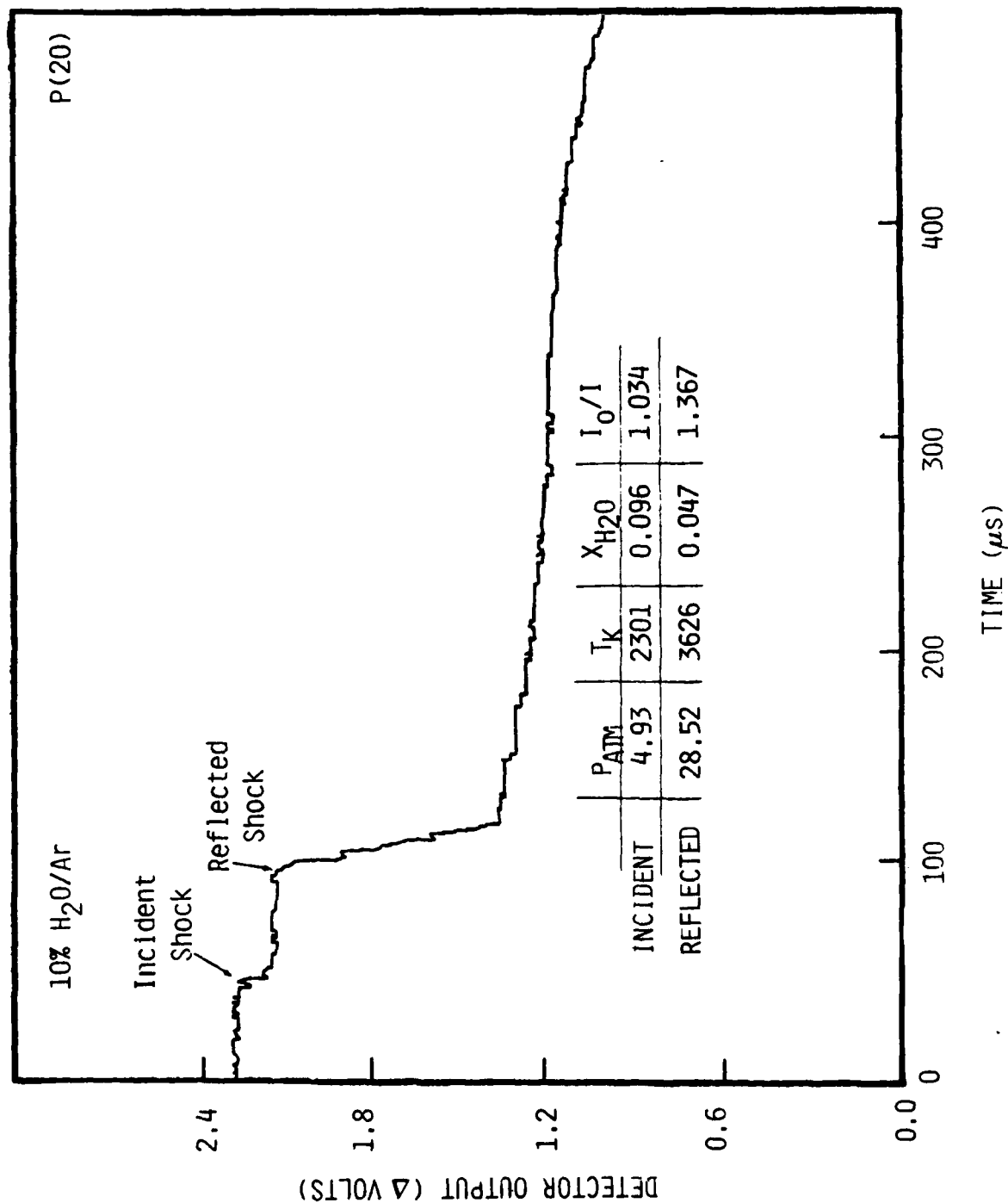


Fig. 14 Typical high temperature laser absorption trace.

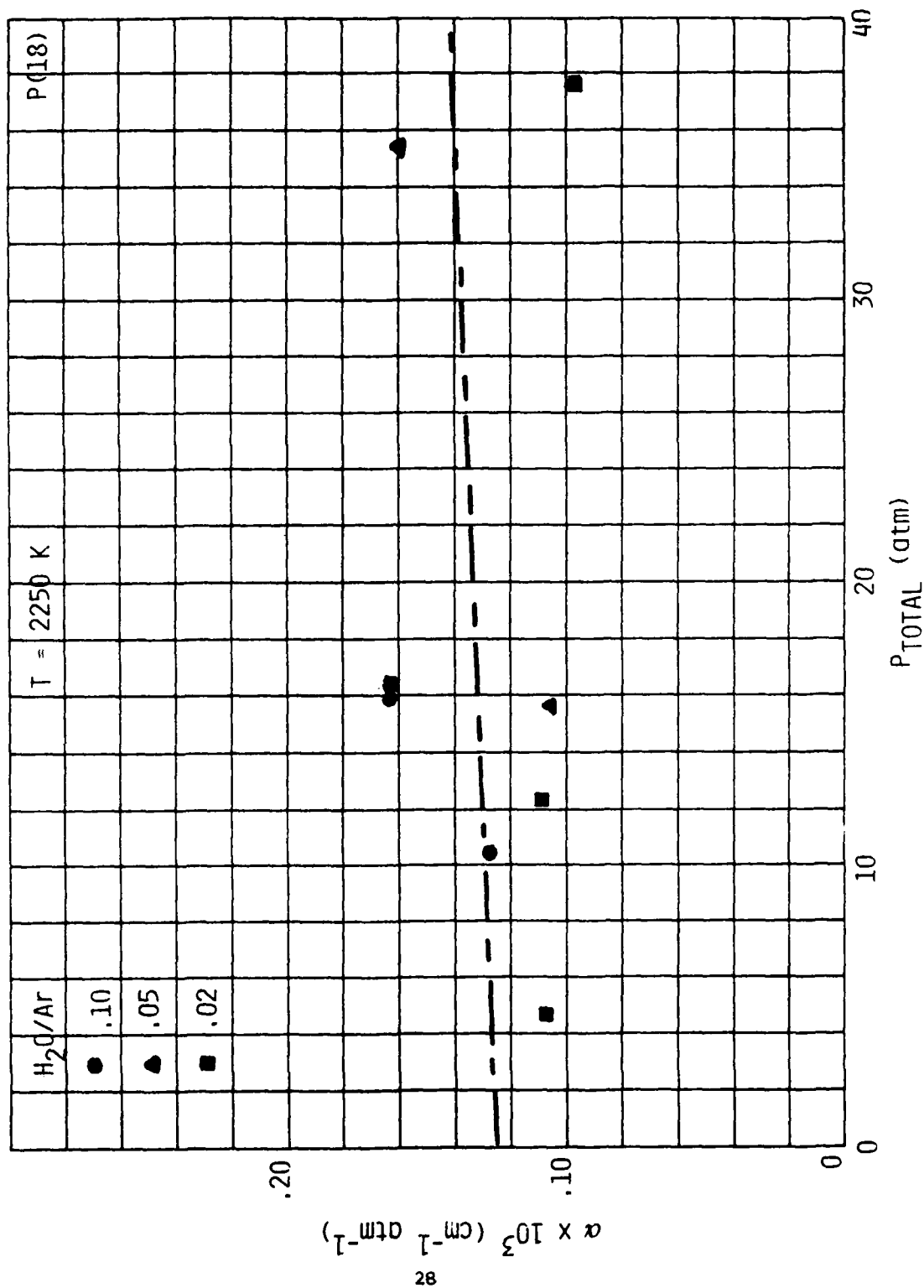


Fig. 15 Absorption versus total pressure on P(18) laser line.

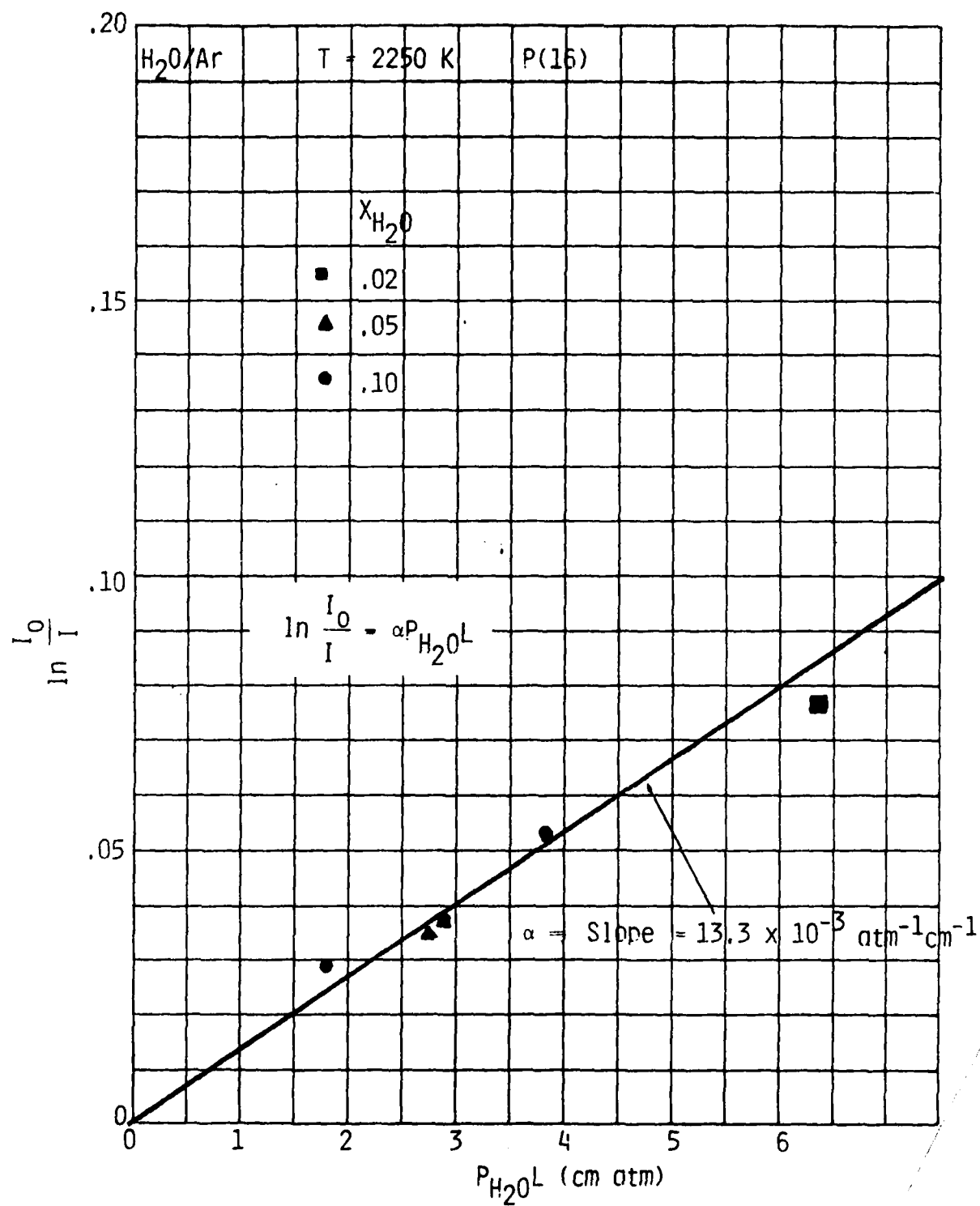


Fig. 16 Absorption versus pressure of water for P(16) laser line.

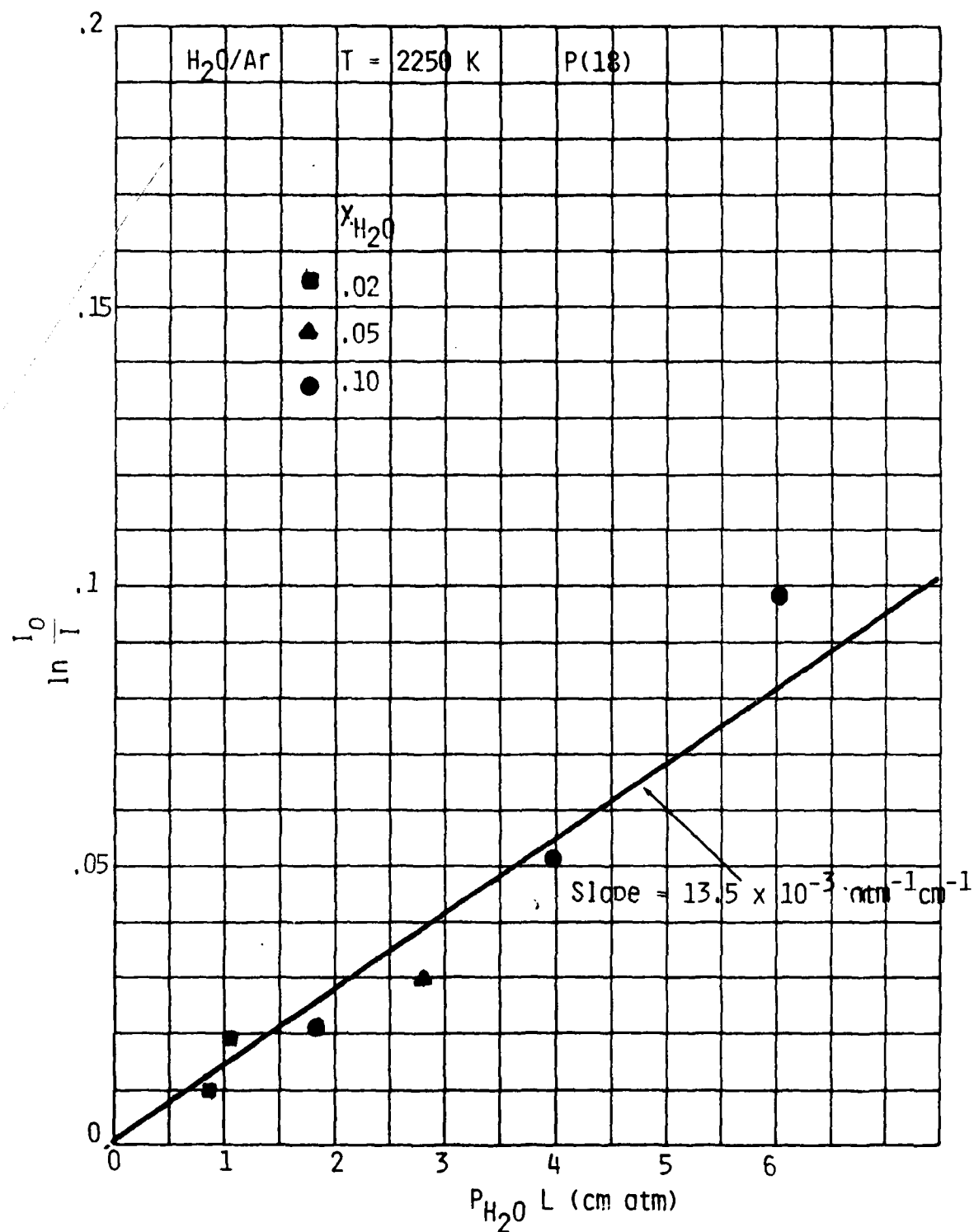


Fig. 17 Absorption versus pressure of water for P(18) laser line.

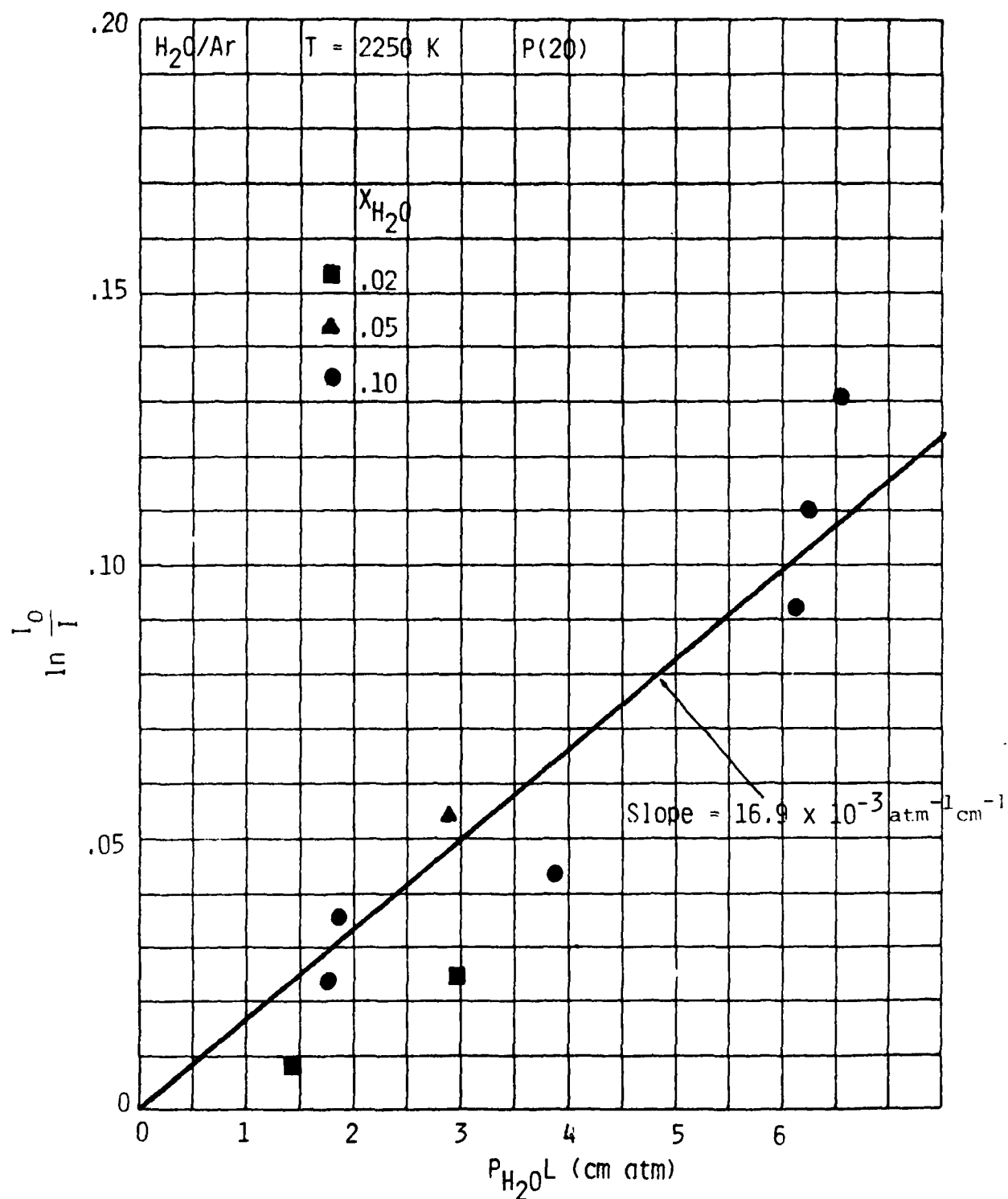


Fig. 18 Absorption vs. pressure of water for P(20) laser line.

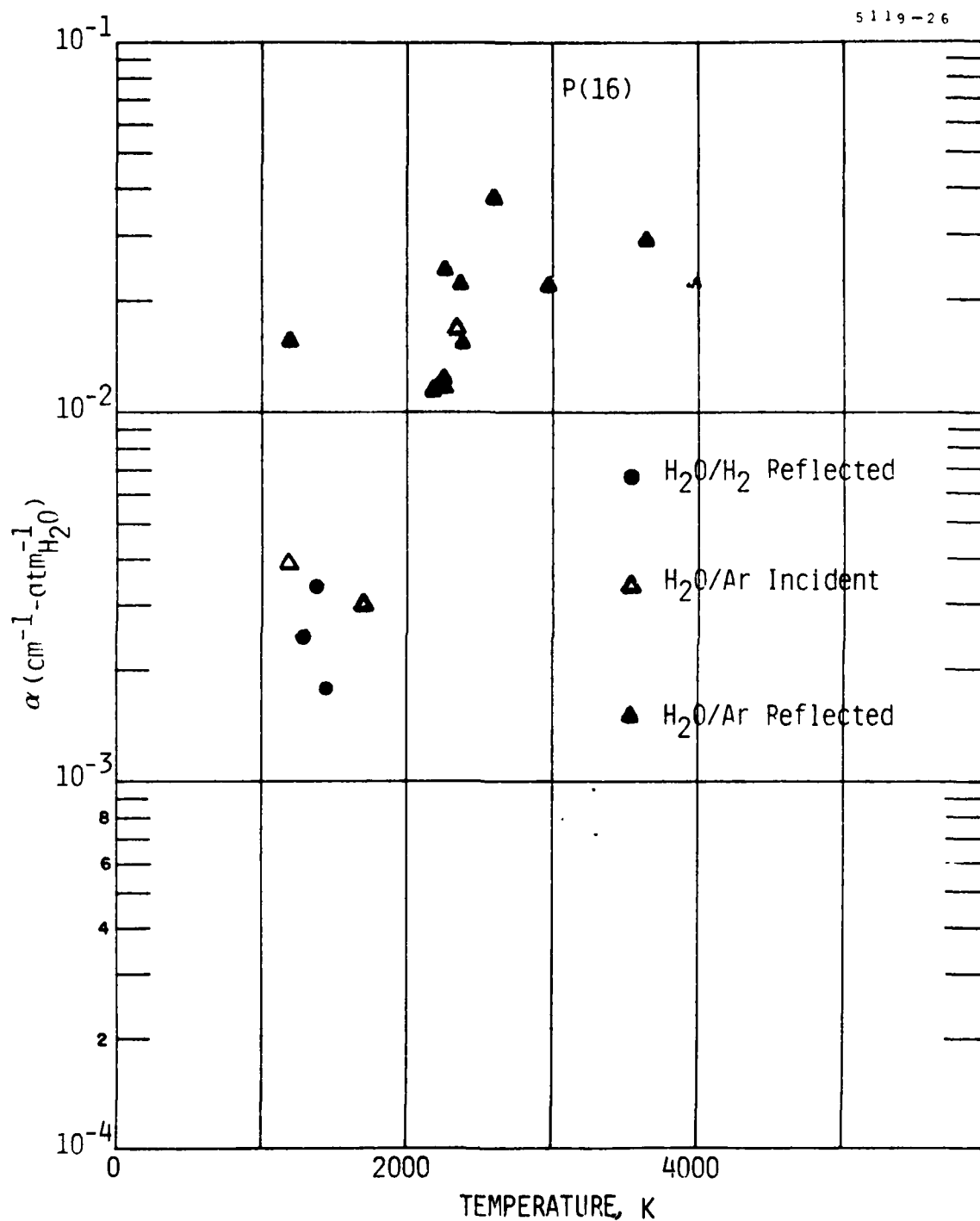


Fig. 19 Absorption coefficient vs. temperature for P(16) laser line.

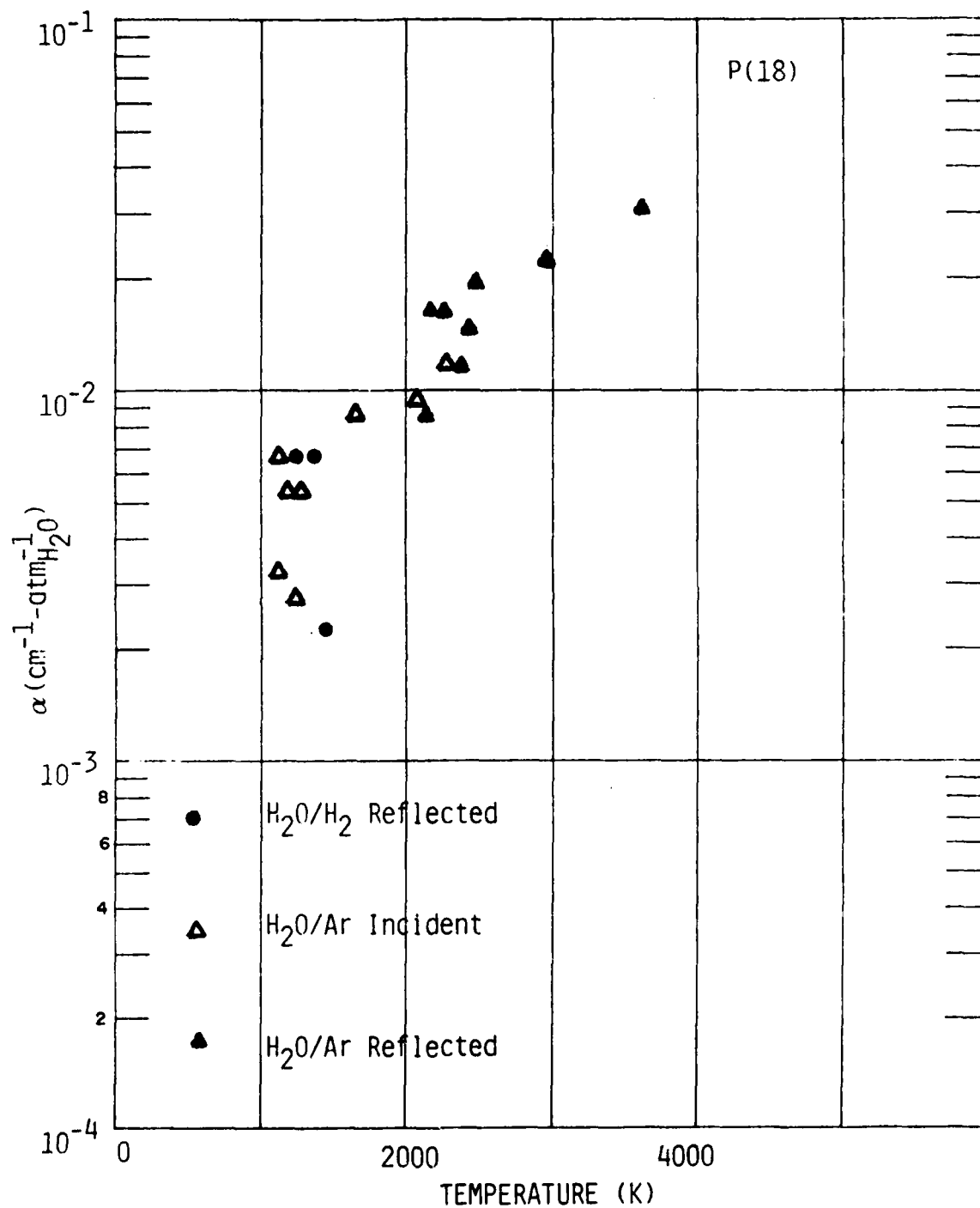
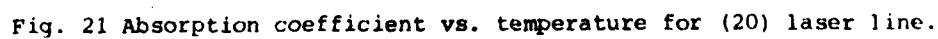


Fig. 20 Absorption coefficient vs. temperature for P(19) laser line.



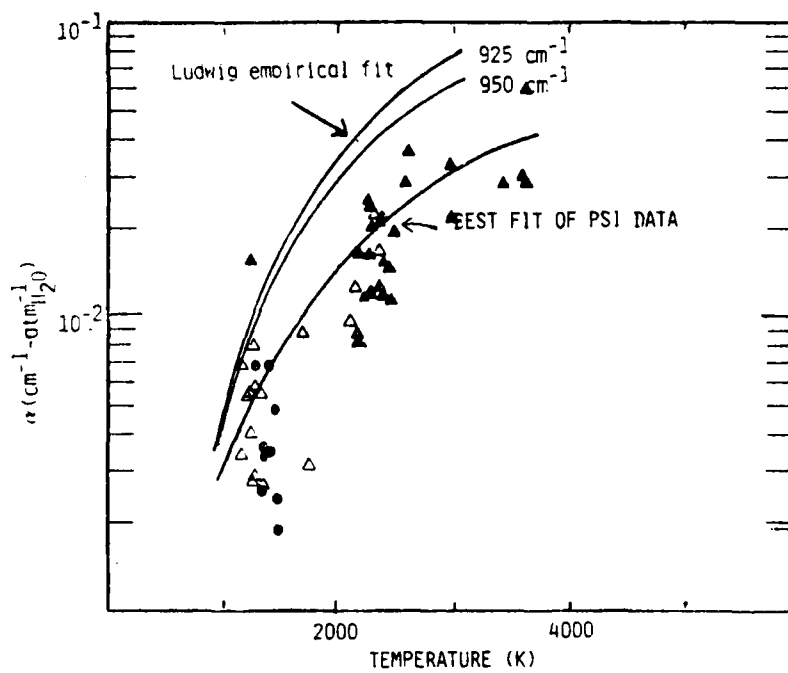


Fig. 22 Water absorption coefficient versus temperature.

6. DISCUSSION

The experimental observation that changes in total gas pressure, the partial pressure of the water, or the collision partner, along with small changes in the laser wavelength, do not significantly change the value of the absorption coefficient of H₂O vapor/gas mixtures over the ranges of pressures and temperatures encompassed by these measurements is not surprising for the following reason.

A continuum absorption will be obtained at any temperature if the lines involved in the absorption are broadened into each other. As the temperature rises the density of states increases so that the degree of broadening required to complete the overlap decreases.

The positions of the high temperature water lines are not known with sufficient accuracy to allow a line by line calculation of the absorption coefficient. Ludwig and his coworkers have conducted many measurements of water vapor emission from plumes and flames,⁸ empirically correlated all available low resolution spectra,^{9,10} and obtain an expression for the temperature and pressure dependence of the absorption coefficient averaged over a 25 cm⁻¹ spectral range.

The band model used by Ludwig determines an average rotational line spacing vs. temperature as shown in Fig. 23. His equation for the average spacing as a function of temperature is $d(T) \text{ cm}^{-1} = \exp(-0.00106 T_K + 1.21)$. The primary broadening mechanism under the experimental conditions is collisional broadening. The collisional broadening parameters for all the species of interest are known at room temperature,¹¹ and using these values it is a simple matter to approximate the pressure required to broaden a line to an extent that the linewidth ν_L equals the average line spacing \bar{d} . Above this pressure the absorption will be a continuum. These plots for the gases tested in the study are shown as Fig. 24.

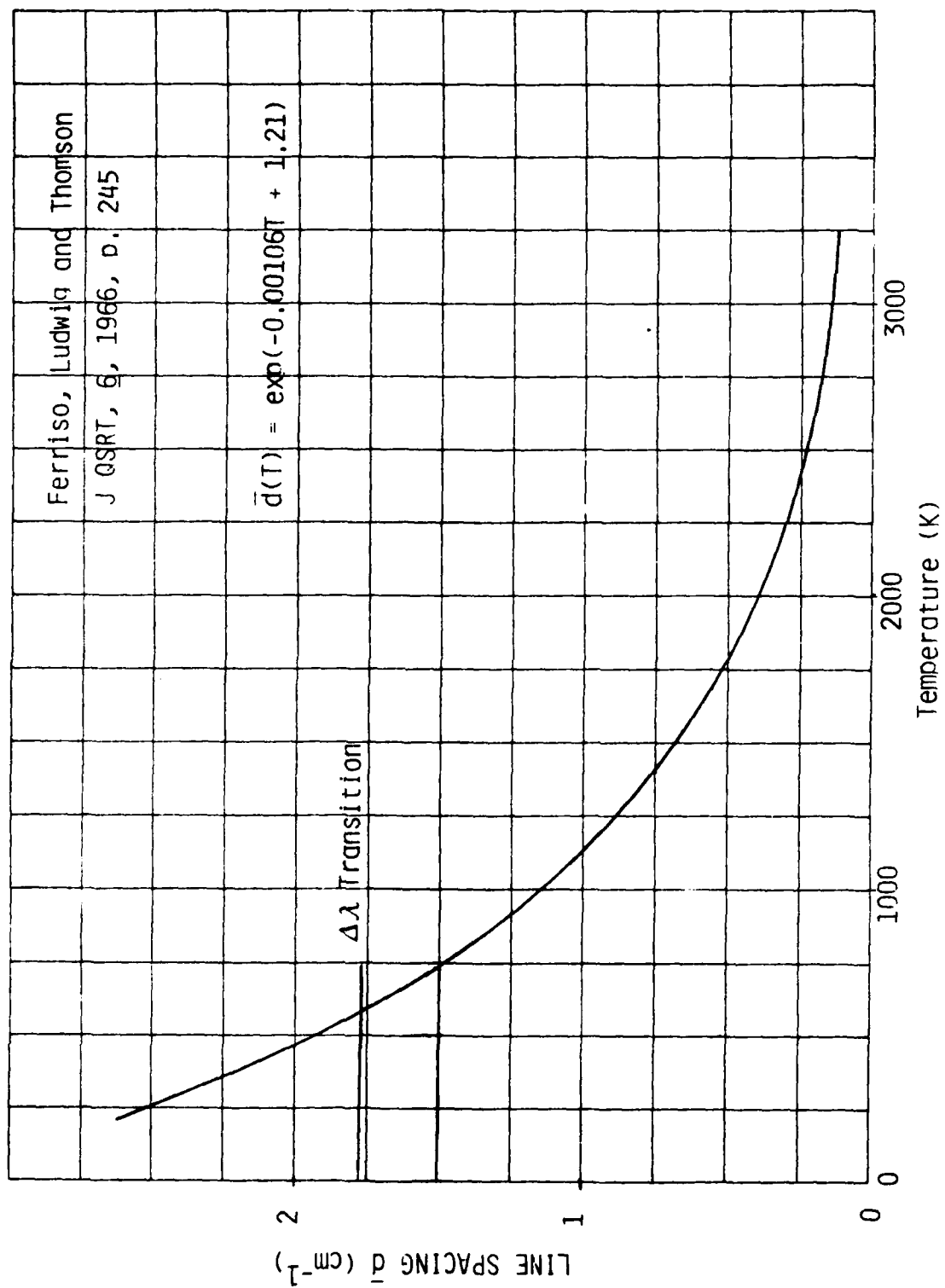


Fig. 23 Band model average rotational line spacing vs temperature

For the pressure conditions required in the operation of a CW laser-heated thruster, this simple approach predicts sufficient broadening to assume a continuum absorption mechanism. Our data closely approximates a curve 50% lower than Ludwig's empirical fit. This is not unexpected either since there is some structure in the high temperature water spectra in the 10.6 micron region. Low resolution spectra recorded in the $944\text{--}948\text{ cm}^{-1}$ region of the spectra appear to be slightly below Ludwig's averaged value; however the respective high resolution spectra could have varied in either direction.

No absorption was observed below 1000 K. This results from a combination of short path length, low pressure, and low absorption coefficients. In several other measurements it has been observed that the absorption coefficient increases quadratically with increasing pressure. This continuum-like phenomenon has been attributed to absorption by water dimers. The weakly bound complexes dissociate as the temperature increases, and their dissociation is suppressed by increasing pressure. The functional form of the low temperature absorption has been described by Roberts and coworkers.¹⁴ Combining our high temperature experimental measurements fitted to a value 50% of Ludwig's predictions, and Roberts low temperature observations, a plot of the temperature dependence of the absorption coefficient of H_2O can be generated for all possible operating regimes of a CW laser-heated thruster. This plot is shown in Fig. 25.

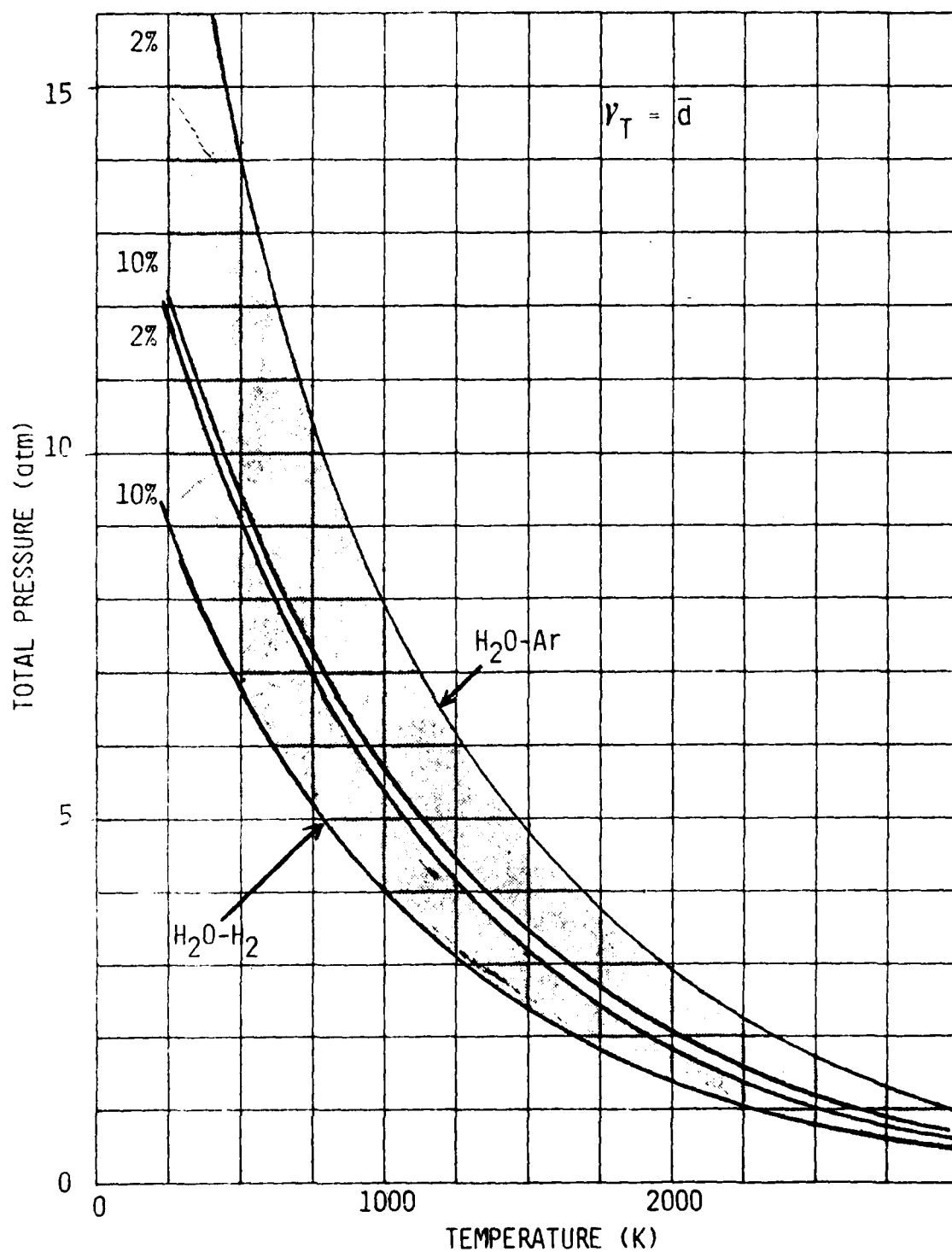


Fig. 24 Calculated collision broadening boundaries for test gas mixtures versus temperature.

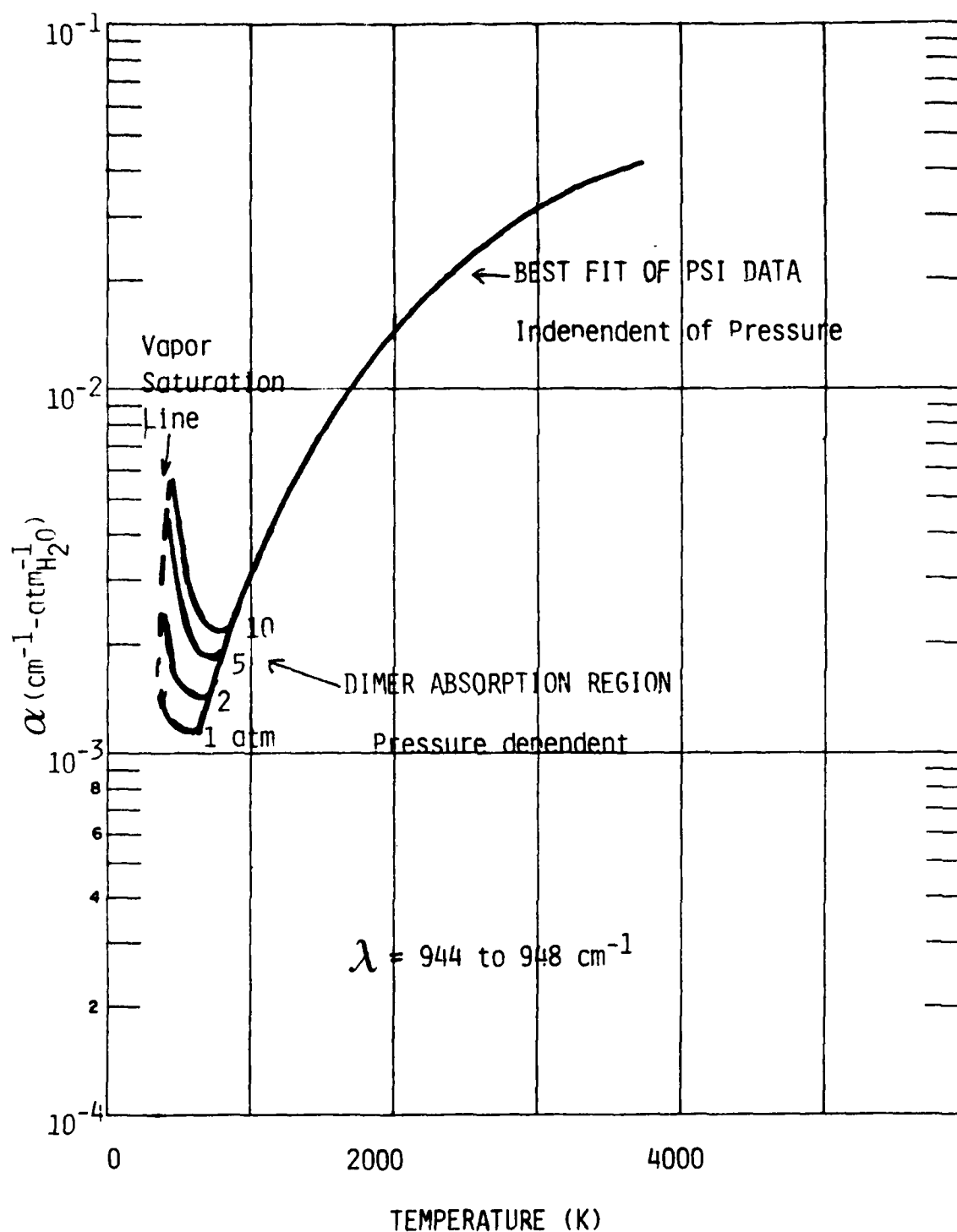


Fig. 25 PSI recommended values for H_2O absorption coefficient.

7. WATER AS AN ABSORBER IN THE CW ROCKET

The low value of the absorption coefficient of water below 1500 K indicates that a laser heated thruster using a simple H_2O/H_2 propellant system may have a startup problem. This will not be known until it is possible to design and test a laboratory scale thruster. The reason is that the presence of liquid water droplets in the gas stream will cause a significant increase in the absorption coefficient, and it might be possible to heat the propellant in a rather short absorption chamber by superheating the droplets and generating the steam at a temperature where the gas phase water absorbs strongly.

If we neglect the potential start up problem, we can investigate the performance of a prototype laser heated thruster using the PSI laser heated thruster codes.¹⁵ Figure 26 indicates the specific impulse and absorption length for a variety of H_2O/H_2 propellant ratios. The diagonal family of curves represent the absorption lengths required for various propellant mixtures vs chamber pressure. The gas is assumed to be either at 3500 or 4000 K. The more horizontal family of curves represents the specific impulse obtained under these conditions. This figure indicates that a reasonably compact thruster operating at 3500 to 4000 K and above 10 atmospheres pressure can yield specific impulses around 1000 s.

The laser power required and absorption chamber heating loads for a small 2 cm radius laser heated thruster are shown in Fig. 27. This figure shows that with a 30-50 kW CW CO_2 laser system, this size thruster will produce 1 pound of thrust with an average heating load of only 40 to 80 W/cm². This is not an unreasonable power level for state of the art CO_2 lasers, thus demonstration experiments for a 1 pound thruster can in principal be conducted.

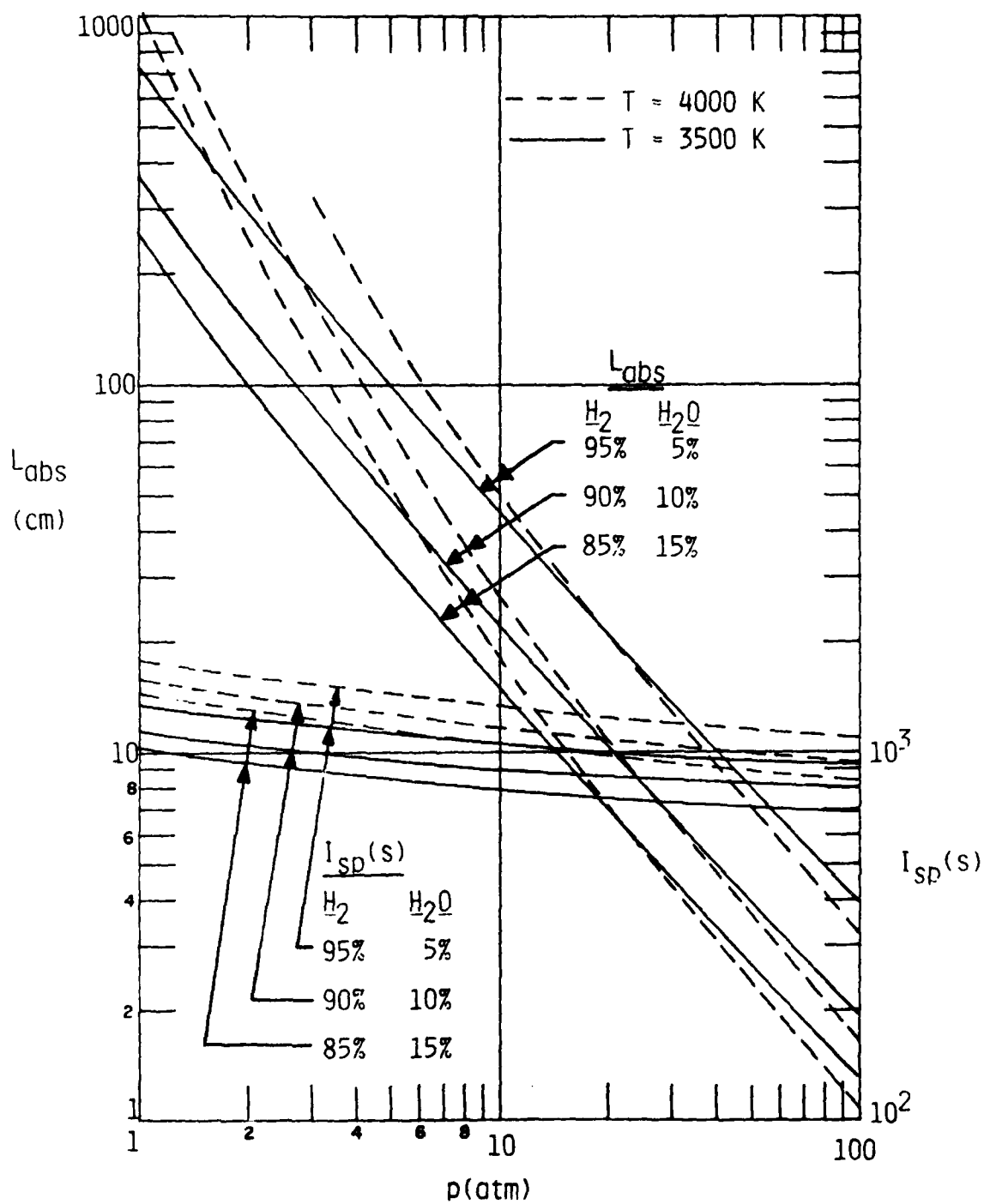
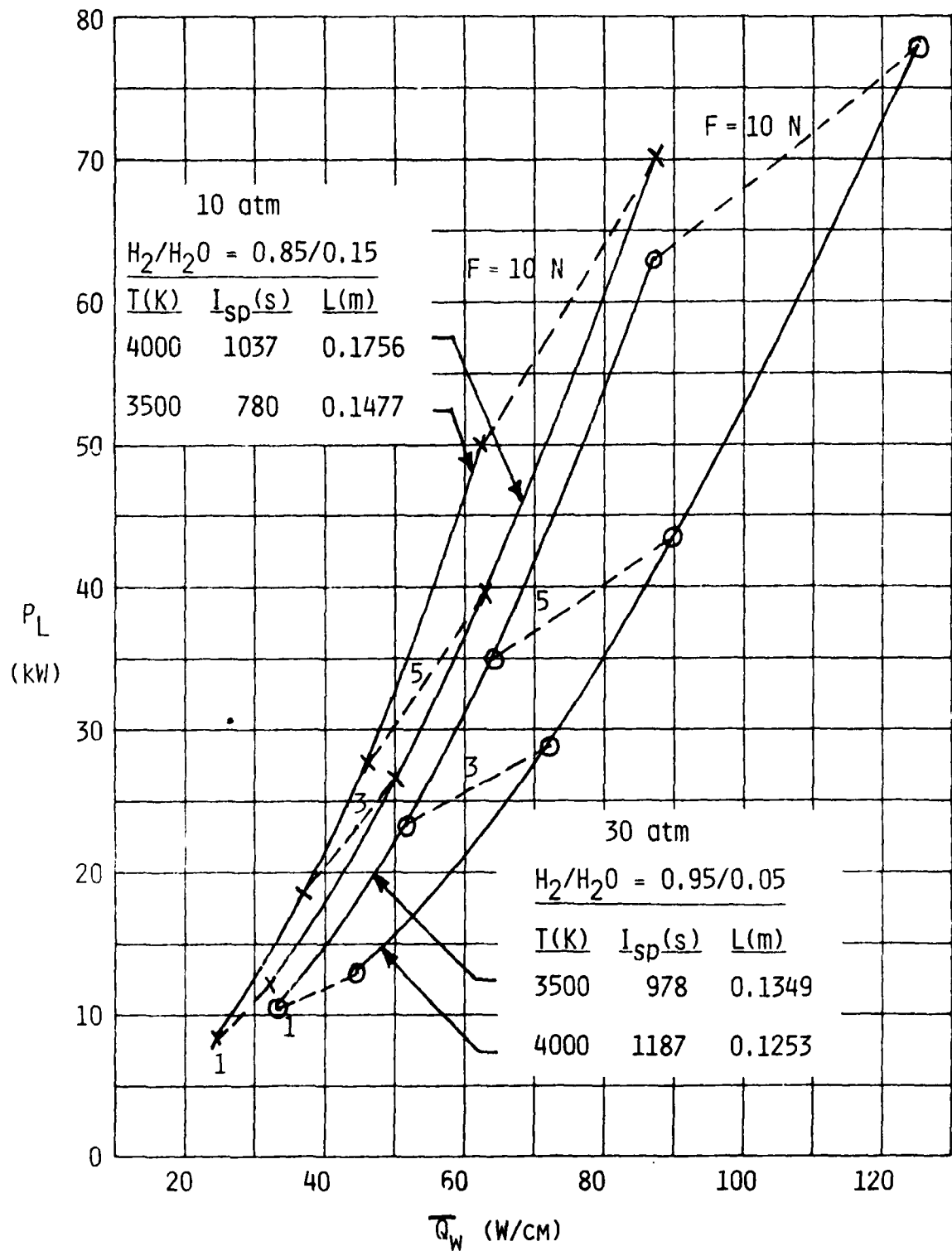


Fig. 26 Absorption length (L_{abs}) and specific impulse (I_{sp}) for H_2/H_2O mixtures vs. total chamber pressure.



8. AMMONIA AS A PROPELLANT AND ABSORBER

As stated in the previous section, there might be a start up problem in a laser heated thruster using an H_2O/H_2 propellant system. In anticipation of this possibility, we have reviewed the available experimental data for ammonia, a molecule which strongly absorbs CO_2 laser radiation at room temperature.

Room temperature laser absorption coefficient measurements of ammonia have been conducted for the laser transitions of interest⁷. The absorption coefficients are: $\alpha_P(16) = 0.12$, $\alpha_P(18) = 0.14$, and $\alpha_P(20) = 0.49 \text{ cm}^{-1} \text{ atm}^{-1}$. The only high temperature laser absorption measurements found are those conducted at UTRC⁴ and their values are used in the following discussion.

It is desirable to use NH_3 as the propellant in a CW laser heated thruster because NH_3 is easily stored as a liquid and leads to a product ($N_2 + 3H_2$) with a low average molecular weight. If the NH_3 remains intact at higher temperatures, it could serve as an effective low temperature absorber. However, an equilibrium calculation of the mole fraction of NH_3 resulting from an initially pure NH_3 gas, shown in Fig. 28, indicates that from an equilibrium standpoint, NH_3 does not exist in appreciable quantities at temperatures above 1000 K. Therefore, only if the heating process remains nonequilibrium, will the NH_3 remain intact. The kinetics for the decomposition of NH_3 are reasonably well known and are fairly slow at temperatures below 3000 K.

We have performed several calculations to determine the rate of decomposition of NH_3 at various temperatures and pressures in order to make a preliminary assessment of its use as a low temperature absorber. If NH_3 could exist in significant quantities to temperatures where absorption by H_2O could

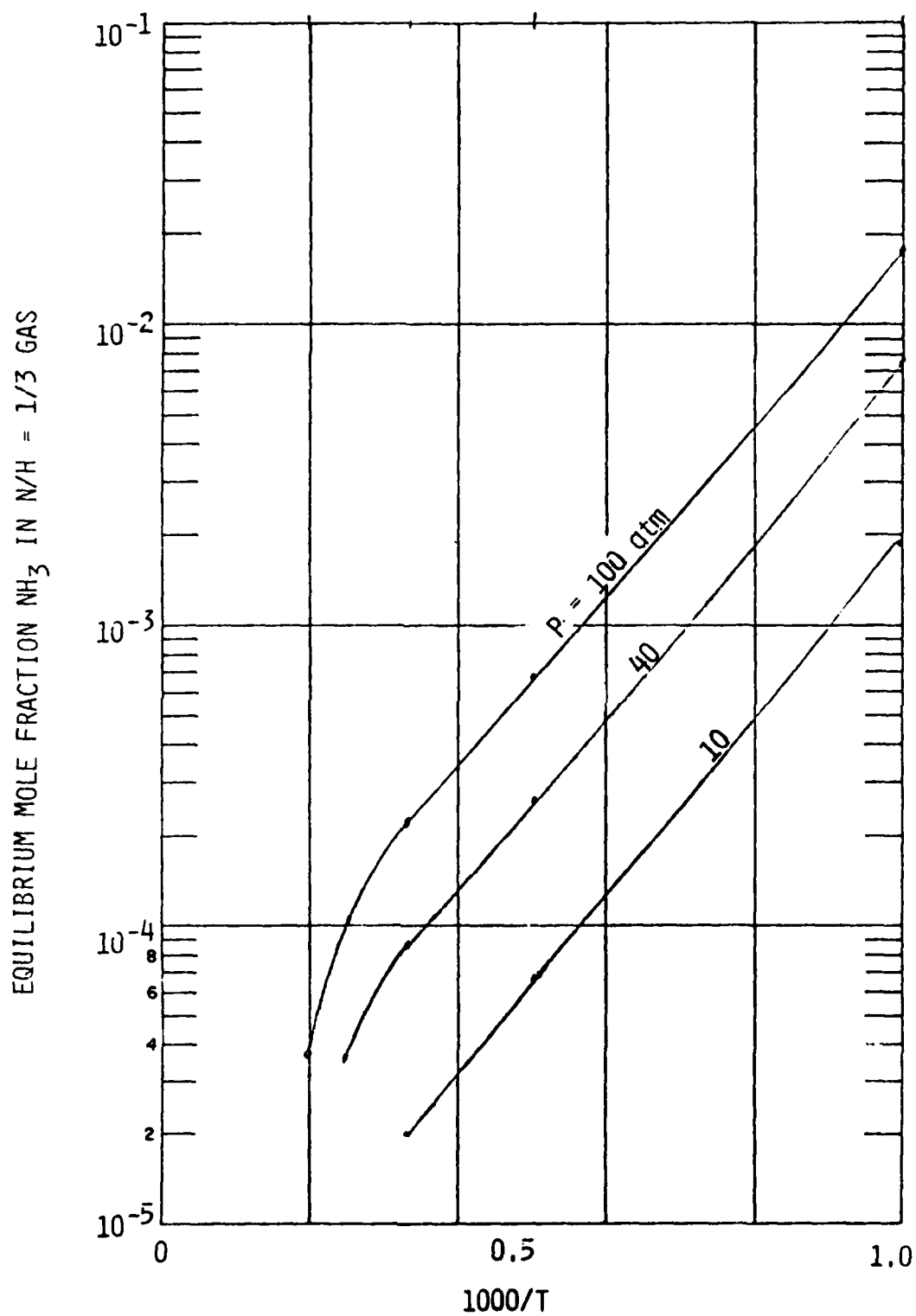


Fig. 28 Equilibrium Concentration of NH_3

take over, NH_3 would indeed be a useful propellant additive. In Fig. 29 we show the results of these calculations where we have calculated the time history of the NH_3 concentration after sudden heating (such as in a shock tube) to various temperatures at various pressures.

The solid curve shows the NH_3 history at 10 atmospheres and 3000 K. In these calculations we have made the area of the flow constant; the gas cools rapidly to 2500 K due to the initial breakup of the NH_3 to form radicals. The rate of removal of NH_3 after about 1 μs is controlled by the reaction



which is limited by the low concentration of nitrogen atoms. At higher pressure (40 atm) the rate of removal is even slower as seen from the dashed curve in Fig. 29. This is because the nitrogen atom concentration is in quasi-steady state with N_2 and is thus reduced by a factor of the square root of the pressure. With the addition of 10% water, the rate of NH_3 removal is increased by a factor of two as is shown by the dash-double-dot curve. This is due to the introduction of a new mechanism



This mechanism still depends upon the presence of nitrogen atoms so that it will scale in the same way as the decomposition without H_2O .

At 2000 K the decomposition rate is very slow. This is indicated in Fig. 29 by the circle at 10 ms. At 4000 K the NH_3 decomposition rate is fast as is indicated by the dash-dot curve. From these curves we can expect that

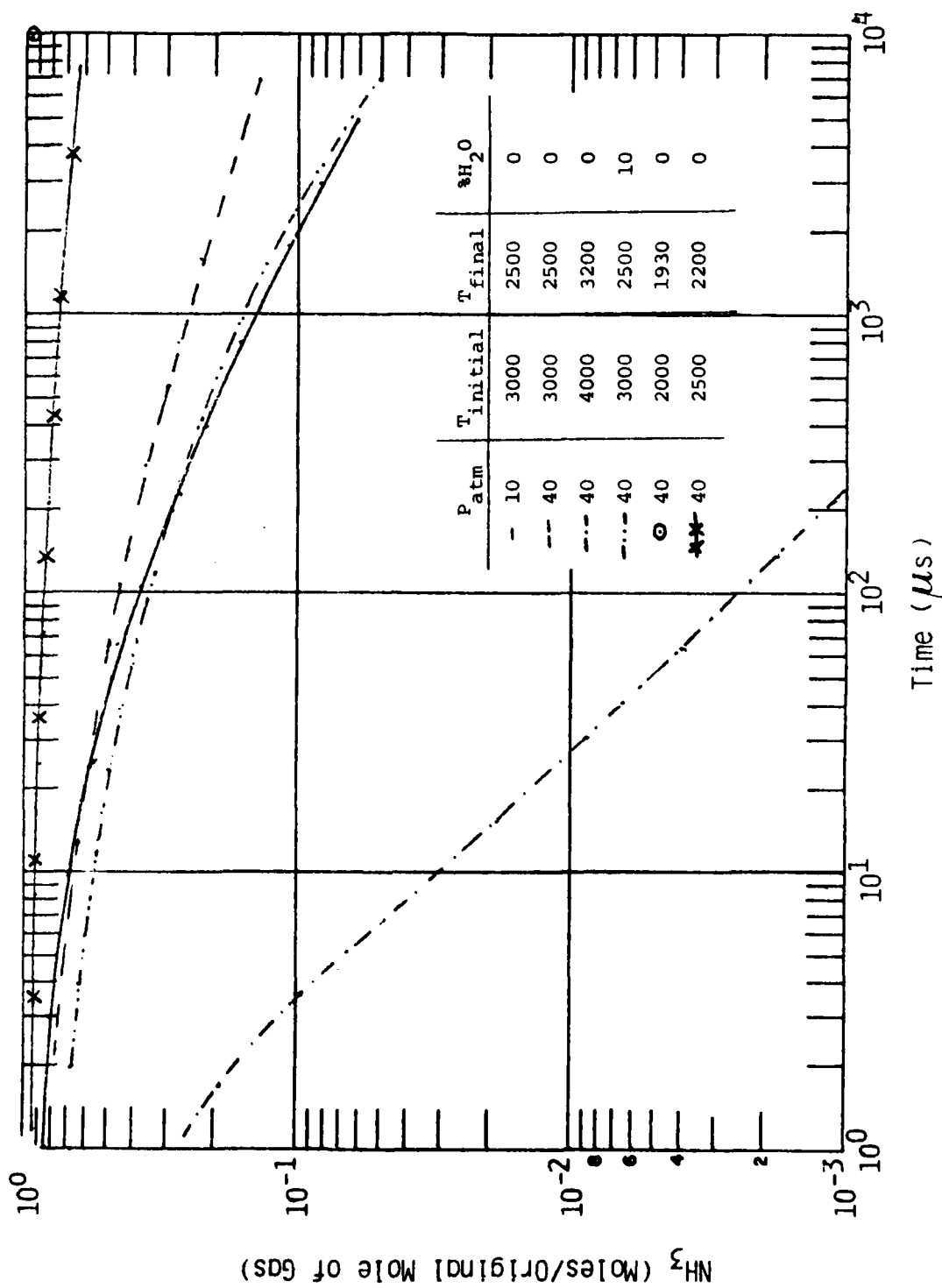


Fig. 29 - NH_3 Decomposition After Sudden Heating.

for a device with a characteristic heating time of about 1 ms, the absorption due to NH_3 would drop off slowly below 2500 K and rapidly above 3000 K. This is qualitatively what was seen in the experiments of Fowler, et al,⁴ at UTRC. The results of their experiments are reproduced in Fig. 31. The rise in the absorption at temperatures above 1000 K is not understood but could be due to the increase in the population of absorbing hot bands of NH_3 or radicals. The fall is undoubtedly due to equilibration of the composition.

With the kinetics of NH_3 dissociation established in Fig. 29, we would like to compare the dissociation time to the flow time in the heating region of a laser-heated thruster to determine if NH_3 would make an effective absorber when used in a thruster. An estimate of the flow time at a temperature level in a laser-heated thruster can be made by combining the flow velocity expected with the absorption length.

Suppose we have a thruster operating to produce a thrust Th at a given specific impulse I_{sp} . Then the mass flow rate is $m = Th/g I_{sp}$ where g is the gravitational constant. If A is the thruster cross sectional area and ρ the density at the cross section of interest, then the velocity there is

$$u = Th/(g I_{sp} \rho A)$$

The absorption coefficient may be expressed as an absorption cross-section σ times the number density of NH_3 , call it n . Thus

$$k = \sigma n = \sigma \rho / m$$

where m is the mass of an ammonia molecule. By combining u and k we obtain the flow time

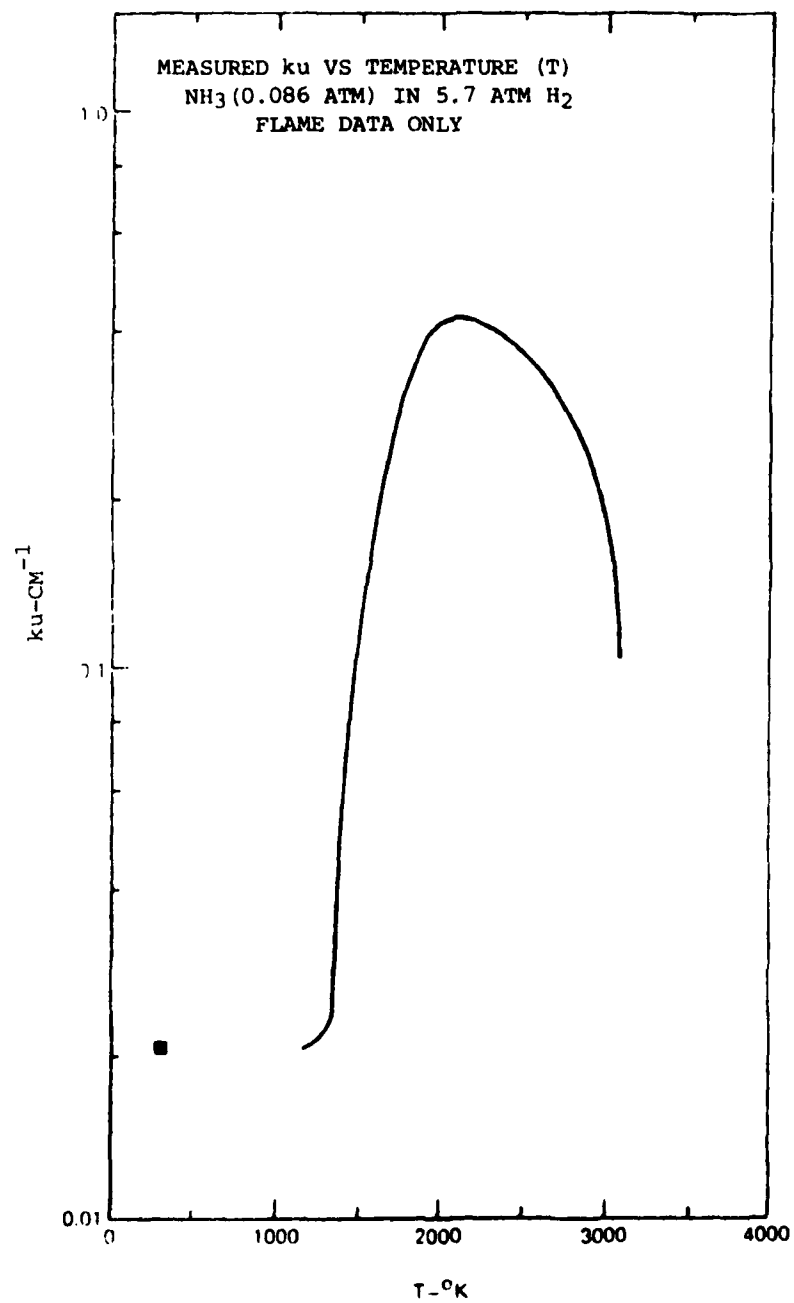


Fig. 30 UTRC⁴ measured NH_3 absorption.

$$t = \frac{1}{uk} = \frac{\pi R^2 m g I_{sp}}{\sigma Th}$$

where R is the cross-section radius. This time is seen to be independent of pressure, but depends on temperature through the absorption cross-section σ . It is directly proportional to area (R^2), and I_{sp} , and inversely proportional to thrust, Th. High thrust decreases the time and large area or I_{sp} increases it.

To make an estimate for NH_3 we need to find σ . For this, we use Fig. 30 of Ref. 4, reproduced as Fig. 31 here. This is a plot of the calculated absorption coefficient of 1 atm of NH_3 in 10 atm of H_2 . The upper curve is for a frozen mixture, and so is only sensitive to the pressure of NH_3 . The following table gives the values of k from the upper curve of Fig. 31, the number density of 1 atm of NH_3 , and their ratio $\sigma = k/n$, against temperature.

<u>T(10³K)</u>	<u>k(cm⁻¹)</u>	<u>n(cm⁻³)</u>	<u>σ(cm²)</u>
0.3	0.61	2.45×10^{19}	2.49×10^{-20}
1	0.35	7.34×10^{18}	4.77×10^{-20}
2	0.070	3.67×10^{18}	1.91×10^{-20}
2.5	0.032	2.94×10^{18}	1.09×10^{-20}
3	0.014	2.45×10^{18}	5.72×10^{-21}
4	0.0037	1.84×10^{18}	2.02×10^{-21}
5	0.0011	1.47×10^{18}	7.49×10^{-22}
6	0.00035	1.22×10^{18}	2.78×10^{-22}

The mass of an ammonia molecule is 2.85×10^{-23} g so the expression for t becomes

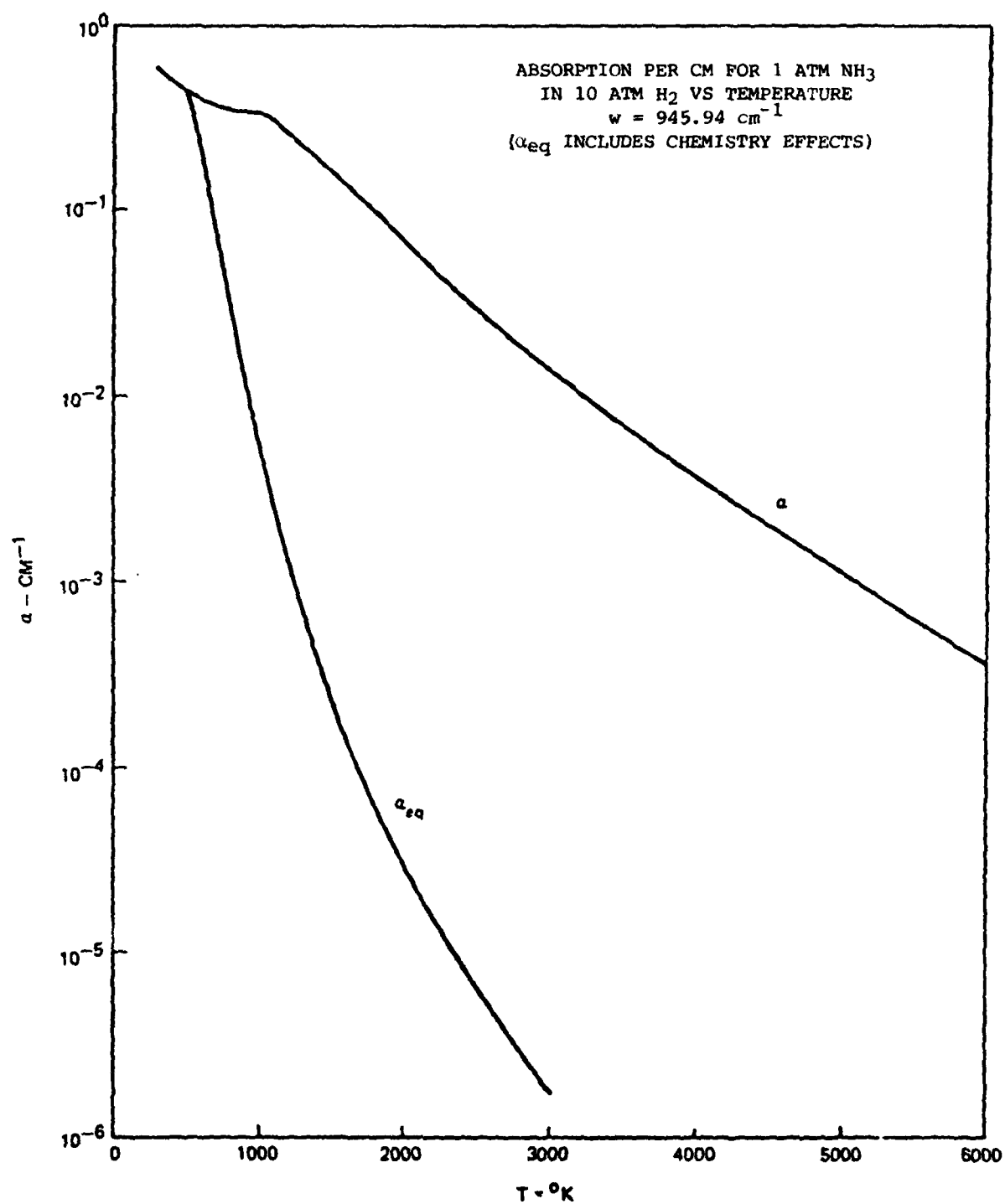


Fig. 31 UTRC⁴ calculated NH_3 absorption coefficient.

$$t = \frac{8.8 \times 10^{-20} R^2}{\sigma} \frac{I_{sp}}{Th}$$

where σ is in cm^2 , R is in cm and Th is in dynes, while t and I_{sp} are in seconds. This can be used to estimate the flow time in a thruster of radius R , thrust Th , and specific impulse I_{sp} , at the temperature where the absorption cross-section for ammonia is σ .

As an example, consider a thruster developing 100 pounds thrust (4.45×10^7 dynes) at a specific impulse of 1000 s. Then

$$t = 2 \times 10^{-24} R^2 / \sigma$$

Using the values for σ from the above table, we find

<u>T(10³K)</u>	<u>t/R²(s/cm²)</u>	<u>R=1 cm</u>	<u>R=3 cm</u>
		<u>t(s)</u>	<u>t(s)</u>
1	4.2×10^{-5}	4.2×10^{-5}	3.8×10^{-4}
2	1.0×10^{-4}	1.0×10^{-4}	9.0×10^{-4}
2.5	1.8×10^{-4}	1.8×10^{-4}	1.6×10^{-3}
3	3.5×10^{-4}	3.5×10^{-4}	3.2×10^{-3}
4	9.9×10^{-4}	9.9×10^{-4}	8.9×10^{-3}

At 3000 K Fig. 30 and the above table indicate that the NH_3 would be more than 60% dissociated for this thruster if it had a radius of 1 cm, while it would be 90% dissociated if it had a radius of 3 cm. However, at 2500 K, it is only 20% dissociated for a radius of 1 cm and 30% dissociated for a radius of 3 cm. So it appears that the kinetics of NH_3 decomposition is slow

enough that NH_3 will remain intact and be an effective low temperature absorber up to 2500 K.

Based upon the above discussion we conclude that ammonia in a laser powered thruster might serve as an effective absorber during the early heating phases. Since water vapor is not a good absorber at low temperatures (<1500 K) and ammonia is, a $\text{NH}_3/\text{H}_2\text{O}/\text{H}_2$ mixture is attractive as a $10.6 \mu\text{m}$ radiative absorber that operates from room temperature to 4000 K, where water vapor is the absorber above 2500 K.

9. SUMMARY AND CONCLUSIONS

No significant variation in the H_2O absorption coefficient was observed as a function of laser wavelength, water concentration, total pressure, or collision partner within the narrow spectral range from 944 to 948 cm^{-1} covered in the measurements. These observations suggest that the water lines are sufficiently broadened to act as a continuum absorber under conditions to be found in a laser-heated rocket thruster. The laser-measured high temperature absorption coefficients are 50 percent lower than the value obtained from the Ludwig empirical curve fit to low resolution data.

For a practical CW laser-heated thruster it is estimated that a propellant absorption coefficient of $10^{-2}\text{ atm}^{-1}\text{-cm}^{-1}$ will be required.^{3,4,15} The absorption coefficient of water vapor does not reach this value until the gas temperature exceeds $1500\text{--}1700\text{ K}$. High temperature operation will not present problems, but there could be a potential start-up problem for a simple $\text{H}_2\text{O}/\text{H}_2$ propellant system, and other low temperature absorbers may be required.

Ammonia absorbs CO_2 laser radiation strongly from room temperature to around 2500 K . Although equilibrium calculations predict substantial dissociation at elevated temperatures, the kinetics suggests that the decomposition of ammonia below 2500 K is sufficiently slow as to make NH_3 a very attractive low temperature absorber. Addition of NH_3 will eliminate any low temperature start up problems. A tertiary propellant mixture, $\text{NH}_3/\text{H}_2\text{O}/\text{H}_2$, therefore should absorb CO_2 laser radiation effectively from room temperature to above 4000 K .

REFERENCES

1. Caledonia, G. E., Wu, P. K., and Pirri, A. N., "Radiant Energy Absorption Studies for Laser Propulsion," Physical Sciences Inc., PSI TR-20 (NASA CR-134809), 1975.
2. Huberman, M., Sellen, J. M., Benson, R., Davenport, W., Davidheiser, R., Mulmud, P., and Glatt, L., "Investigation of Beamed Energy Concepts for Propulsion," TRW Final Report, Contract F04611-76-C-003, AFRPL-TR-76-66, Vols. I and II and AFRPL-TR-76-07, Vol. III, October 1976.
3. Kemp, N. H., Root, R. G., Wu, P. K., Caledonia, G. E., and Pirri, A. N., "Laser-Heated Rocket Studies," Physical Sciences Inc., PSI TR-53, (NASA DR-135127), 1976.
4. Fowler, M. C., Newman, L. A., and Smith, D. C., "Beamed Energy Coupling Studies," Final Technical Report for Contract No. F04611-77-C-0039, AFRPL-TR-79-51, September 1979.
5. Nebolsine, P. E., Pirri, A. N., Goela, J. S., Simons, G. A. and Rosen, D. I., "Pulsed Laser Propulsion," Paper VI-2, AIAA Conference on Fluid Dynamics of High Power Lasers, Cambridge, MA, 1978 (also PSI TR-142).
6. Weiss, R. F., Pirri, A. N., and Kemp, N. H., Astronautics and Aeronautics, March 1979, p 50-58.
7. Patty, R. R., Russwurm, G. M., McClenny, W. A., and Morgan, D. R., "CO₂ Laser Absorption Coefficients for Determining Ambient Levels of O₃, NH₃, and C₂H₄," Applied Optics, Vol. 13, No. 12, December 1974, p. 2852.
8. Ludwig, C. G., "Measurements of the Curves-of-Growth of Hot Water Vapor," Applied Optics, Vol. 10, No. 5, May 1971, pp 1057-1073.
9. Ferriso, C. C., Ludwig, C. B., and Thomson, A. L., "Empirically Determined Infrared Absorption Coefficients of H₂O from 300 to 3000 K," J. Quant. Spectrosc. Radiat. Transfer, Vol. 6, pp 241-273 Pergamon Press Ltd., 1966, Great Britain.
10. Ludwig, C. B., Ferriso, C. C., Malkmus, W., and Boynton, F. P., "High-Temperature Spectra of the Pure Rotational Band of H₂O," J. Quant. Spectrosc. Radiat. Transfer, Vol. 5, pp 697-714, Pergamon Press Ltd., 1965, Great Britain.
11. Penner, S. S. and Varanasi, P., "Spectral Absorption Coefficients in the Pure Rotation Spectrum of Water Vapor," J. Quant. Spectrosc. Radiat. Transfer, Vol. 7, pp 687-690, Pergamon Press Ltd., 1967, Great Britain.

12. Varanasi, P., Chou S., and Penner, S. S., "Absorption Coefficients for Water Vapor in the 600-1000 cm^{-1} Region," J. Quant. Spectrosc. Radiat. Transfer, Vol. 8, pp. 1537-1541, Pergamon Press Ltd., 1968, Great Britain.
13. Roberts, R. E., Selby, J. E. A., and Biberman, L. M., "Infrared Continuum Absorption by Atmospheric Water Vapor in the 8-12 μm Window," Applied Optics, Vol. 15, No. 9, September 1976, pp 2085-2090.
14. Kemp, N. H. and Krech, R. H., "Laser-Heated Thruster, Final Report," Physical Sciences Inc., TR-220, September 1980.
15. Peterson, J. C., Thomas, M. E., Nordstrom, R. J., Damon, E. K., and Long, R. K., "Water Vapor-Nitrogen Absorption at CO_2 Laser Frequencies," Applied Optics, Vol. 18, No. 6, 15 March 1979, pp. 834-841.
16. Peterson, J. C., Thomas, M. E., Nordstrom, R. J., Damon, E. K., and Long, R. K., "Water Vapor-Nitrogen Absorption at CO_2 Laser Frequencies," Applied Optics, Vol. 18, No. 6, March 1979.

DATE
ILME